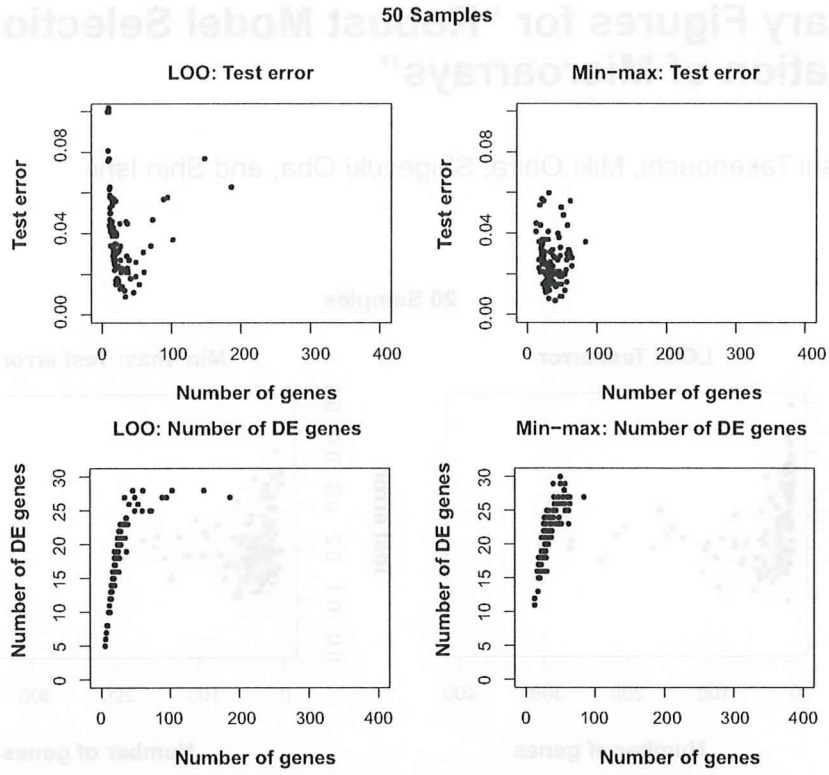

Figure S2. Distributions of test errors and numbers of selected true DE genes for various numbers of selected genes for T-WV classifiers based on 50 artificial samples

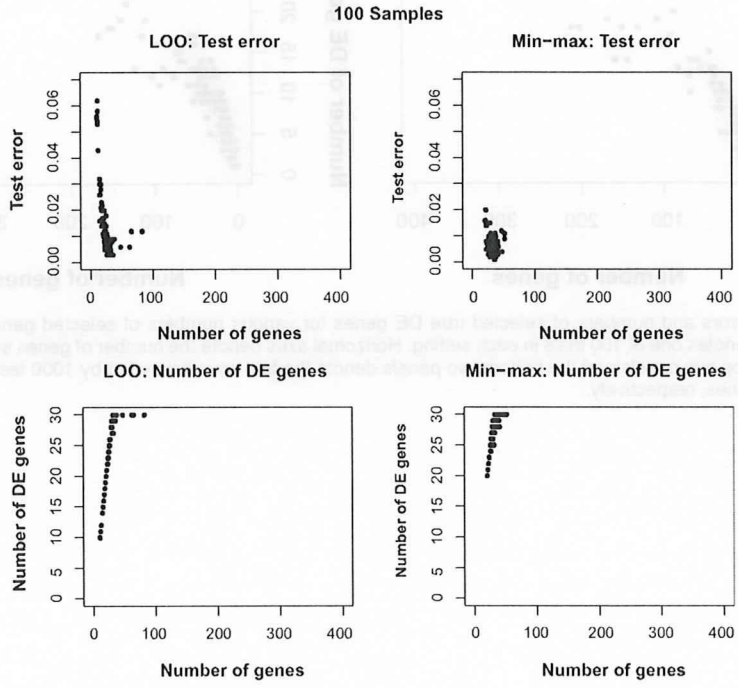

Figure S3. Distributions of test errors and number of selected true DE genes for various numbers of selected genes for T-WV classifiers based on 100 artificial samples.

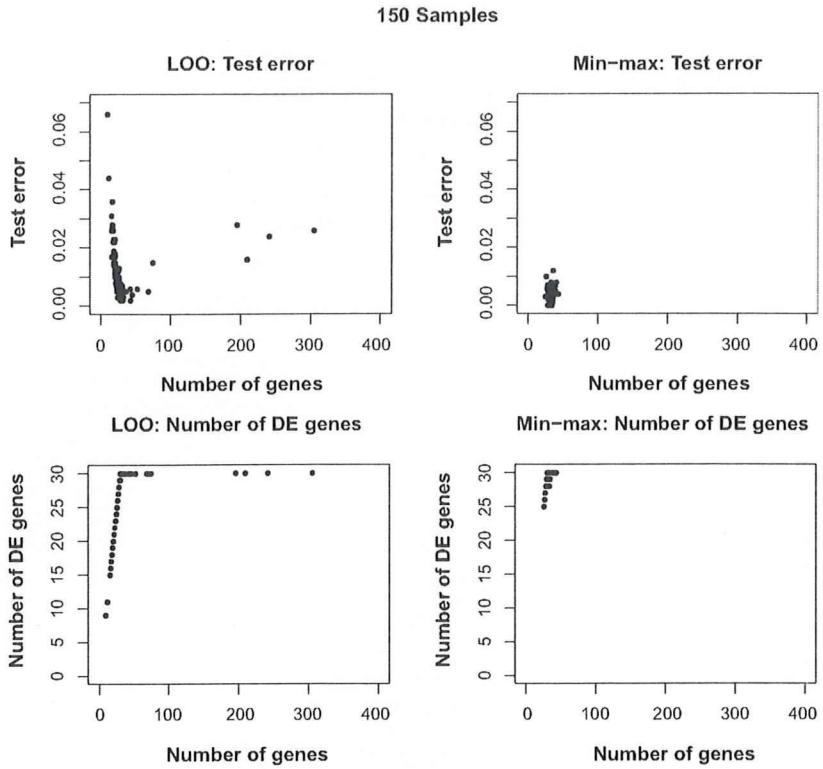

Figure S4. Distributions of test errors and number of selected true DE genes for various numbers of selected genes for T-WV classifiers based on 150 artificial samples.

High expression of *ncRAN*, a novel non-coding RNA mapped to chromosome 17q25.1, is associated with poor prognosis in neuroblastoma

MENG YU[1,2], MIKI OHIRA[1], YUANYUAN LI[1], HIDETAKA NIIZUMA[1], MYAT LIN OO[1], YUYAN ZHU[1,3,4], TOSHINORI OZAKI[1], ERIKO ISOGAI[1], YOHKO NAKAMURA[1], TADAYUKI KODA[3], SHIGEYUKI OBA[5], BINGZHI YU[2] and AKIRA NAKAGAWARA[1]

[1]Division of Biochemistry and Innovative Cancer Therapeutics, Chiba Cancer Center Research Institute, Chiba 260-8717, Japan; [2]Department of Biochemistry and Molecular Biology, China Medical University, Shenyang 110001, P.R. China; [3]Research Center for Functional Genomics, Hisamitsu Pharmaceutical Co., Inc., Chiba 260-8717, Japan; [4]Department of Urology, No. 1 Hospital, China Medical University, Shenyang 110001, P.R. China; [5]Integrated Systems Biology Laboratory, Department of Systems Science, Graduate School of Informatics, Kyoto University, Kyoto 611-0011, Japan

Received October 14, 2008; Accepted December 16, 2008

DOI: 10.3892/ijo_00000219

Abstract. Neuroblastoma shows complex patterns of genetic aberrations including *MYCN* amplification, deletion of chromosome 1p or 11q, and gain of chromosome 17q. The 17q gain is frequently observed in high-risk neuroblastomas, however, the candidate genes still remain elusive. In the present study, we integrated the data of comparative genomic hybridization of 236 tumors by BAC array and expression profiling of 136 tumors by using the in-house cDNA microarray carrying 5,340 genes derived from primary neuroblastomas. A novel candidate gene mapped to chromosome 17q25.1 with two splicing variants, *Nbla10727* and *Nbla12061*, was identified. The transcript size appeared to be 2.3 kb by Northern blot, however, the cDNA sequences had no obvious open reading frame. The protein product was undetectable by both *in vivo* and *in vitro* translation assays, suggesting that the transcript might not encode any protein product. Therefore, we named it as *ncRAN* (non-coding RNA expressed in aggressive neuroblastoma). In analysis of 70 patients with sporadic neuroblastoma, the high levels of *ncRAN* mRNA expression were significantly associated with poor outcome of the patients ($p<0.001$). The multivariate analysis showed that expression of *ncRAN* mRNA was an independent prognostic factor among age, stage, origin and *MYCN* expression. Ectopic expression of *ncRAN* induced transformation of NIH3T3 cells in soft agar, while knockdown of endogenous *ncRAN* with RNA interference significantly inhibited cell growth in SH-SY5Y cells. Collectively, our results suggest that *ncRAN* may be a novel non-coding RNA mapped to the region of 17q gain and act like an oncogene in aggressive neuroblastomas.

Correspondence to: Dr Akira Nakagawara, Division of Biochemistry and Innovative Cancer Therapeutics, Chiba Cancer Center Research Institute, 666-2 Nitona, Chuo-ku, Chiba, Chiba 260-8717, Japan
E-mail: akiranak@chiba-cc.jp

Key words: neuroblastoma, non-coding RNA, ncRAN, prognosis

Introduction

Neuroblastoma is one of the most common pediatric solid tumors in children and originates from sympathoadrenal lineage of the neural crest. Its clinical behavior is heterogeneous because the tumors often regress spontaneously when developed in patients under one year of age, while they grow rapidly and cause very poor clinical outcome when occurring in patients over one year of age (1). Recent cytogenetic analyses have revealed that given subsets of neuroblastoma with unfavorable prognosis often have *MYCN* amplification, gains of chromosome 1q, 2p, and 17q as well as allelic losses of 1p, 3p, and 11q (1). However, the precise molecular mechanisms underlying pathogenesis and progression of neuroblastoma still remain unclear.

Accumulating evidence shows that gain of chromosome 17 or 17q is the most frequent genetic abnormality in neuroblastoma (1-4). We have previously conducted microarray-based comparative genomic hybridization (array-CGH) with a DNA chip carrying 2,464 BAC clones to examine genomic aberrations in 236 primary neuroblastomas (5). Our array-CGH analysis demonstrated three major groups of genomic aberrations in sporadic neuroblastomas (n=112) that can well define the prognoses of neuroblastomas: a genetic group of silent chromosomal aberration (GGS, 5-year cumulative survival rate: 68%), a genetic group of partial chromosomal gains and/or losses (GGP, 43%), and a genetic group of whole chromosomal gains and/or losses (GGW, 80%). The classification of three genetic groups corresponded well with the pattern of chromosome 17 abnormalities, namely, no gain of either chromosome 17 or 17q, gain of chromosome

17q, and gain of whole chromosome 17, respectively (5). Thus, 17q gain has been implicated in close correlation with aggressiveness of neuroblastoma (5-7). The region has been narrowed down to 17q21-qter, in which several important candidate genes such as *Survivin* and *PPM1D* were suggested to be involved in acquiring aggressiveness of neuroblastoma (4,7,8).

In the present study, by combining with our previous array-CGH data, we searched for the candidate 17q gain gene(s) by applying the results of our gene-expression profiling obtained from the analysis of 136 neuroblastoma samples using an in-house cDNA microarray carrying 5,340 genes isolated from primary neuroblastomas (9,10). This approach has led us to identify a novel non-coding RNA as the candidate mapped to the region of chromosome 17q gain. Its high expression is significantly associated with aggressiveness of primary neuroblastomas.

Materials and methods

Patients. Tumor specimens were collected from the patients with neuroblastoma who had undergone biopsy or surgery at various institutions in Japan. Two hundred and thirty-six and 136 tumor samples were used for array-CGH and expression profiling, respectively (5,10). Among them, sporadic cases were 112 and 70, respectively. The clinical stage of tumor was classified according to the INSS criteria (11). Expression data for the latter 70 sporadic neuroblastomas, which were composed of 15 stage 1, 8 stage 2, 17 stage 3, 25 stage 4, and 5 stage 4s tumors, were used for the Kaplan-Meier analysis. The status of *MYCN* amplification in each tumor had been determined as described previously (8). Patients were treated according to previously described protocols (12,13). The procedure of this study was approved by the Institutional Review Board of the Chiba Cancer Center (CCC19-9).

Microarray-based comparative genomic hybridization (array-CGH) and gene expression profiling. Array-based CGH experiments for 236 neuroblastomas by using a chip carrying 2,464 BAC clones which covers the whole human genome at ~1.2-Mb resolution were performed as described previously (5). For the gene expression profiling of 136 neuroblastomas, we employed an in-house cDNA microarray, carrying 5,340 cDNAs obtained from the oligo-capping cDNA libraries generated from anonymous neuroblastoma tissues (10,14-16). The array-CGH and gene expression profile data are available at NCBI Gene Expression Omnibus (http://www.ncbi.nlm.nih.gov/geo/) with accession numbers GSE 5784 and GSE 5779, respectively.

Cells, culture and transfection. NIH3T3, COS7 and human neuroblastoma cell lines were cultured in Dulbecco's modified Eagle's medium (DMEM) or RPMI-1640 medium containing 10% (vol/vol) heat-inactivated fetal bovine serum (FBS) and antibiotics. Cultures were maintained in a humidified atmosphere containing 5% CO_2 at 37˚C. COS7 and NIH3T3 cell lines were transiently transfected using Lipofectamine 2000 reagent (Invitrogen, Carlsbad, CA, USA) according to the manufacturer's protocol.

Construction of expression plasmid. The full-length cDNAs of *Nbla10727* and *Nbla12061* were cloned from the established full length-enriched cDNA libraries which we made from the primary neuroblastomas as described (14-16). The full-length cDNAs were then inserted into pcDNA3 or pcDNA3-FLAG plasmids.

In vitro transcription and translation assay. In vitro translation was carried out in the presence of [^{35}S]-methionine using TNT T7 Quick coupled transcription/translation system (Promega, Madison, WI, USA) according to the manufacturer's instructions. The products were resolved by SDS-PAGE and detected by autoradiography.

In vivo [^{35}S]-labeling experiment. COS7 cells were transfected with the FLAG-tagged *ncRAN* expression vectors or the HA-tagged MEL1 expression plasmid. After 24 h, cells were rinsed with 1X PBS 3 times and recultured in fresh growth medium without methionine and antibiotics. Two hours later, [^{35}S]-methionine (GE Healthcare, Tokyo, Japan) was added to the medium to a final concentration of 0.1 mCi/ml, and cells were further incubated. Cells were harvested and whole cell lysates were subjected to immunoprecipitation using a monoclonal anti-Flag antibody or a polyclonal anti-HA antibody. Immunoprecipitates were resolved by SDS-PAGE and detected by autoradiograph.

RNA isolation and semi-quantitative reverse transcription-PCR (RT-PCR). Total RNA was isolated from frozen tumor tissues by an AGPC method (8). Total RNA (5 μg) was employed to synthesize the first-strand cDNA by means of random primers and SuperScript II reverse transcriptase (Invitrogen) following the manufacturer's protocol. We prepared appropriate dilutions of each single stranded cDNA for subsequent PCR by monitoring an amount of glyceraldehyde-3-phosphate dehydrogenase *(GAPDH)* as a quantitative control. The PCR amplification was carried out for 28 cycles (preheat at 95˚C for 2 min, denature at 95˚C for 15 sec, annealing at 55˚C 15 sec, and extension at 72˚C 20 sec) for *ncRAN* (*Nbla10727* and *Nbla12061*). The primers used were: *ncRAN* (*Nbla10727*) 5'-CAGTCAGCCTCAGTTTC CAA-3' (forward); 5'-AGGCAGGGCTGTGCTGAT-3' (reverse), *ncRAN* (*Nbla12061*) 5'-ATGTTAGCTCCCA GCGATGC-3' (forward); 5'-CTAACTGCCAAAAGGTTT TCC-3' (reverse).

Northern blot analysis. Total RNA (20 μg) was subjected to electrophoresis and Northern blotting. The cDNA insert (*Nbla10727*) was labeled with [α-^{32}P]-dCTP (GE Healthcare) by the BcaBEST™ labeling kit (Takara, Tokyo, Japan) and used for the hybridization probe.

Soft agar assay. NIH3T3 cells were transfected with FLAG-*Nbla10727*, FLAG-*Nbla12061* or empty vector, and resuspended in 0.33% agar (wt/vol) in DMEM with 10% FBS at a density of 500 cells/plate. Cell suspensions were poured on the top of the base layer (0.5% agar (wt/vol) in fresh medium, and grew in a 5% CO_2 incubator for 14 days. Colonies >100 μm were counted under an Olympus microscope.

Table I. The comparison of *ncRAN/Nbla10727/Nbla12061* expression level among three major groups of genomic aberrations in neuroblastomas.

Genetic group	n	*ncRAN* expression Mean ± SD (log2 ratio)	p-value	
ncRAN-long/Nbla10727				
GGS (silent)	n=10	-1.12±0.39	p=0.004	
GGP (partial 17q+)	n=26	-0.60±0.48		p=0.952
GGW (whole 17+)	n=35	-1.11±0.48	p<0.001	
ncRAN-short/Nbla12061				
GGS (silent)	n=10	-1.60±0.33	p=0.070	
GGP (partial 17q+)	n=26	-1.23±0.59		p=0.163
GGW (whole 17+)	n=35	-1.81±0.43	p<0.001	

n, number of samples; GGS, Genetic group silent (normal 17); GGP, Genetic group partial gains/losses (17q gain); GGW, Genetic group whole gains/losses (17 gain); *ncRAN* expression levels are shown as normalized log2 ratio of microarray data. p-values were calculated based on statistical t-test.

RNA interference. Oligonucleotides for knocking down the *ncRAN* with *Sac*I and *Xho*I extension were inserted into pMuni vector. The oligonucleotides used were: 5'-CCC CATCCTCTAGTAGCCACGGTTTCAAGAGAACCGT GGCTACTAGAGGATTTTTTGGAAAC-3' and 5'-TCG AGTTTCCAAAAAATCCTCTAGTAGCCACGGTTCTCT TGAAACCGTGGCTACTAGAGGATGGGGAGCT-3'. The plasmids containing the oligonucleotide sequence were transfected into SH-SY5Y cells by using Lipofectamine 2000 reagent (Invitrogen) according to the manufacturer's protocol.

Statistical analysis. The Student's t-tests were used to explore possible associations between *ncRAN* expression and other factors, such as age. Kaplan-Meier curves were calculated and survival distributions were compared using the log-rank test. Univariate and multivariate analyses were made according to the Cox hazard models. q-value was also calculated because *ncRAN* expression was measured with 5340 genes in the microarray (17). Statistical significance was set at $p<0.05$.

Results

Identification of a novel Nbla10727/12061 gene mapped to chromosome 17q25.1 upregulated in advanced neuroblastomas with gain of chromosome 17q. To explore the candidate genes for therapeutic target against aggressive neuroblastomas, the genomic and molecular characteristics specific to high-risk tumors were surveyed. We previously conducted array-CGH analysis with a microarray carrying 2,464 BAC clones to examine genomic aberrations in 236 primary neuroblastomas and found that the gain of chromosome 17q was most strongly correlated with the patient's prognosis (5). The genetic group of 'silent chromosomal aberrations' (GGS) could be defined as the tumor group without apparent abnormalities in chromosome 17, and the genetic group of 'whole chromosomal gains and/or losses' (GGW) as that with gain of whole chromosome 17 (5-year cumulative survival rate in 112 sporadic neuroblastomas: 68 and 80%, respectively, according to ref. 5). On the other hand, the genetic group of 'partial chromosomal gains and/or losses' (GGP) with gain of chromosome 17q showed poor prognosis (43%).

According to the different grade of aggressiveness among the genetic groups, we hypothesized that the GGP tumors may have higher levels of expression of the activated 17q candidate gene(s) that is (are) involved in defining the grade of malignancy of neuroblastoma than the GGS or GGW tumors. We then used our data set of gene expression profile in 136 neuroblastomas to subtract the genes mapped to the commonly gained region of chromosome 17q and differentially expressed in the GGP tumors at high levels and the GGS or GGW tumors at low levels. Consequently, we found two cDNA clones *Nbla10727* and *Nbla12061* (Fig. 1A) on our in-house microarray carrying 5,340 cDNAs obtained from oligo-capping cDNA libraries generated from different subsets of primary neuroblastomas (10,14-16), both of which were splicing variants of the same gene mapped to chromosome 17q25.1 (Table I and Fig. 1B, expression in GGP more than that in GGS or GGW). Database searching showed that both 2,087-bp and 2,186-bp insert sequences (Genbank/DDBJ accession numbers: AB447886 and AB447887) did not exhibit significant similarity to any previously known genes. As the size of mRNA was ~2.3 kb by Northern blot (Fig. 1C), the clones *Nbla10727* and *Nbla12061* appeared to be almost full-length cDNAs. Therefore, *Nbla10727*/12061 appeared to be the gene activated for its expression in neuroblastomas with partial gain of chromosome 17q, but not activated in those with diploid or triploid pattern of whole chromosome 17.

The *Nbla10727*/12061 gene was expressed in multiple human tissues with preferential expression in heart, kidney, lung, spleen, mammary gland, prostate and liver, but with low expression in neuronal tissues such as brain and cerebellum, fetal brain and adrenal gland (Fig. 1D).

High expression of Nbla10727/12061 is associated with poor prognosis of neuroblastoma. The analysis by semi-quantitative RT-PCR in a panel of cDNAs obtained from 8 favorable (stage 1, <1-year-old, single copy of *MYCN* and high expression

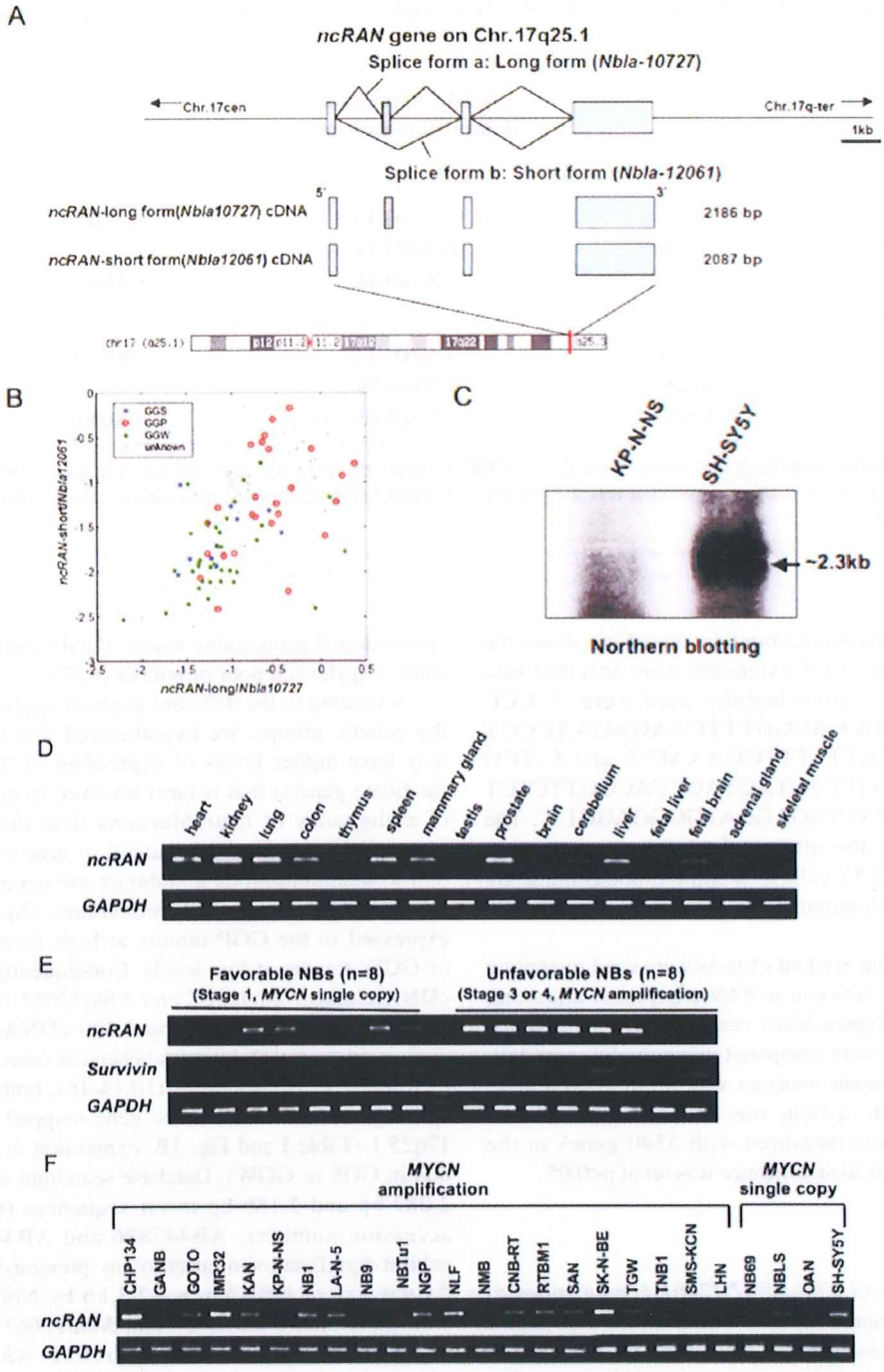

Figure 1. *ncRAN* is mapped to the 17q gain region. A, Genomic structure of *ncRAN* region on chromosome 17q25.1. Splicing variants, whose sequences were contained in cDNAs as *ncRAN-long/Nbla10727* and *ncRAN-short/Nbla12061*, are schematically shown. These are transcribed from a single gene, *ncRAN* (see text). B, High expression of *ncRAN* is associated with high malignant subset of neuroblastoma. Scatter plot of the expression levels of the *ncRAN-long/Nbla10727* and *ncRAN-short/Nbla12061* in 71 primary neuroblastomas with both accompanying expression and aCGH data. Blue, red, green, and black spots denote GGS, GGP, GGW and unknown genomic group samples, respectively. As shown in Table I, the expression levels of the *ncRAN* were significantly higher in GGP tumors (+17q gain) than in GGS (no 17 gain) or GGW (+ whole 17 gain) tumors ($p=0.004$ and $p<0.001$ for *ncRAN-long/Nbla10727*, and $p=0.070$ and $p<0.001$ for *ncRAN-short/Nbla12061*, respectively), whereas their expression levels in GGS and GGW tumors were comparable ($p=0.952$ for *ncRAN-long/Nbla10727*, and $p=0.163$ for *ncRAN-short/Nbla12061*, see also Table I), suggesting that the acquired allele(s) at 17q might be silenced at least for the *ncRAN* expression in GGW tumors, and that high expression of *ncRAN* is associated with high malignant subset of neuroblastoma. C, Northern blot analysis of *ncRAN*. Total RNA (20 μg) prepared from neuroblastoma cell lines, SH-SY5Y and KP-N-NS were used. A 2.3-kb band was visible in only SH-SY5Y cells. The cDNA insert (*Nbla10727*) was labeled with [α-^{32}P]-dCTP and used for the hybridization probe. D, Semiquantitative RT-PCR of *ncRAN* in multiple human tissues and neuroblastoma cell lines. Total RNA of 25 adult tissues and two fetal tissues were purchased from Clontech Co. Ltd. The expression of *GAPDH* is also shown as a control. E, Semi-quantitative RT-PCR of *ncRAN* in favorable and unfavorable subsets of primary neuroblastomas. The mRNA expression patterns for *ncRAN* and *Survivn*, a known oncogene identified at 17q, were detected by semi-quantitative RT-PCR procedure in eight favorable (lanes: 1-8, stage 1, with a single copy of *MYCN*) and eight unfavorable (lanes: 9-16, stage 3 or 4, with *MYCN* amplification) neuroblastomas. F, Semiquantitative RT-PCR of *ncRAN* in neuroblastoma cell lines. Twenty-one neuroblastoma cell lines with *MYCN* amplification and 4 cell lines with a single copy of *MYCN* were used for this study as templates.

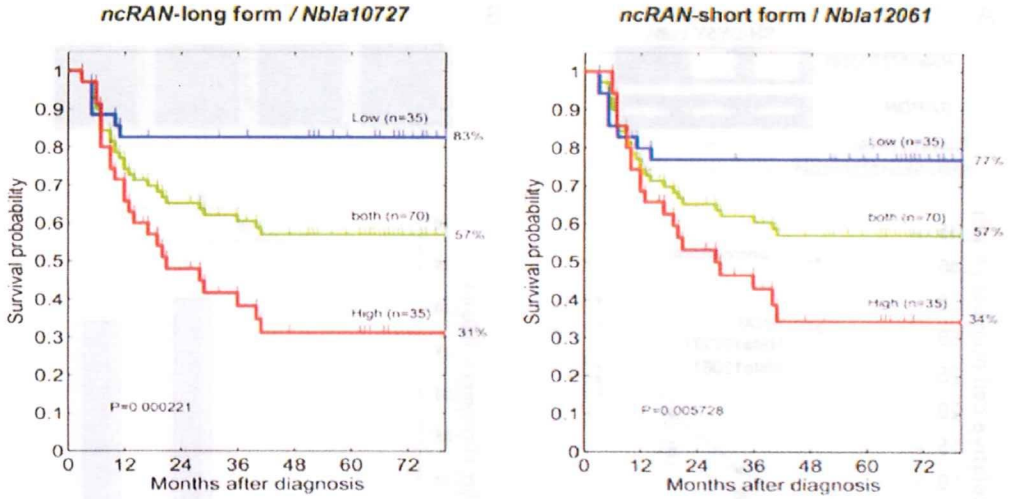

Figure 2. The high expression of *ncRAN/Nbla10727/12061* mRNA is a prognostic indicator of unfavorable neuroblastomas. The Kaplan-Meier survival curves were drawn from the results of the cDNA microarray data of 70 sporadic neuroblastomas (log-rank test, p=0.000221 and p=0.005728, respectively).

of *TrkA*) and 8 unfavorable (stage 3 or 4, >1-year-old, amplified *MYCN* and low expression of *TrkA*) primary neuroblastomas confirmed that this novel gene was expressed at significantly high levels in the latter compared to the former (Fig. 1E), such as *Survivin* which we have previously reported as one of the candidate genes mapped at the region of 17q gain (9). Among neuroblastoma cell lines, high or moderate levels of expression of *Nbla10727/12061* was observed in cell lines with *MYCN* amplification most of which had 17q gain, whereas it was relatively low in those with a single copy of *MYCN* and without the 17q gain (Fig. 1F).

As shown in Fig. 2, our microarray data of 70 sporadic neuroblastomas showed that the high levels of *Nbla10727/12061* expression were significantly associated with poor prognosis (log-rank test, p=0.000221 and p=0.005728, respectively). The multivariate analysis using Cox proportional hazard model demonstrated that expression of *Nbla10727/12061* was an independent prognostic factor among age at diagnosis, disease stage, tumor origin and *MYCN* expression (Table II). Thus, the expression level of *Nbla10727/12061* is a novel prognostic factor of neuroblastoma that is closely associated with gain of chromosome 17q.

Nbla10727/12061 is involved in inducing enhancement of cell growth in neuroblastoma cells and transformation of NIH3T3 cells. To investigate function of *Nbla10727/12061*, we transfected SH-SY5Y neuroblastoma cells with the siRNA, since SH-SY5Y cells have 17q gain in their genome as well as higher mRNA expression of *Nbla10727/12061*. As shown in Fig. 3A, suppression of endogenous levels of *Nbla10727/12061* transcripts significantly inhibited cell growth in SH-SY5Y neuroblastoma cells as compared with the control cells. On the other hand, the soft agar colony formation assay showed that the enforced expression of *Nbla10727/12061* significantly enhanced the anchorage-independent growth of NIH3T3 mouse fibroblast cells (Fig. 3B). These results suggested that *Nbla10727/12061* was a novel candidate gene of the region of 17q gain with an oncogenic function.

ncRAN-Nbla10727/12061 is a large non-coding RNA. Several lines of evidence from the gene structure analysis as well as the comparative genomic analysis described below further suggested that *Nbla10727/12061* is a non protein-coding but functional RNA. We therefore tentatively named this gene as *ncRAN* (non-coding RNA expressed in aggressive neuroblastoma).

First, the full-length cDNA sequences of *ncRAN*, which are suggested to be relevant to both *Nbla10727* and *Nbla12061* cDNAs by Northern blot analysis (Fig. 1C), did not contain any long-enough open reading frames (>200 bp). Bioinformatic analysis indicated that there were no ESTs longer than those two cDNAs at the genomic locus, and that the CpG island was located at the 5' region of the cDNA sequences.

Second, no protein product was translated both *in vivo* and *in vitro* from the *ncRAN* transcripts (Fig. 4). Though only the possible open reading frames (>150 bp) within the *ncRAN* cDNA were from n.t. 190 to 354 (55 amino acids) and from 293 to 469 (59 amino acids) in *Nbla10727*, none of the putative translation start sites contains the Kozak consensus sequence. In addition, these predicted protein products of 55 and 59 amino acids did not exhibit significant similarity to any other known protein or protein domain. Furthermore, *in vivo* transcription and translation of the full-length *ncRAN* did not lead to the synthesis of any peptide or protein (Fig. 4B), though endogenously and ectopically expressed *ncRAN* were easily detectable at mRNA level (Fig. 4A). Coincident with the above observation, the *ncRAN* protein product could not be detected using [^{35}S]-methionine-labeling system *in vitro* (Fig. 4C).

Third, we performed sequence comparison of the *ncRAN* gene with genome sequences of other species and found it has high similarity (>90% identity in nucleotides) with primates including orangutan, chimpanzee and rhesus, but not those with mice and rat (Fig. 5). We also searched for the possible long open reading frames of *ncRAN* homologs in these highly similar species, resulting in failure. The highly conserved sequence similarity only with primates may

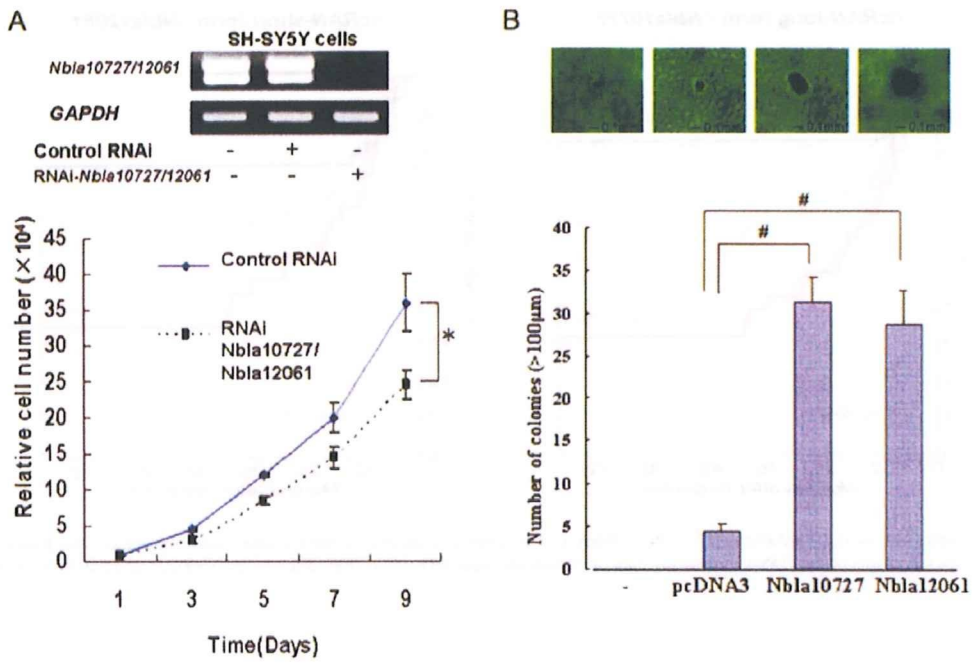

Figure 3. *ncRAN* is involved in inducing enhancement of cell growth in neuroblastoma cells and transformation of NIH3T3 cells. A, Knockdown of *ncRAN* suppress cell growth in SH-SY5Y neuroblastoma cells. SH-SY5Y cells were transfected with expression plasmid for siRNA against *ncRAN* termed pMuni-si*Nbla10727* or with the empty plasmid. On day 2, total RNA was prepared from the cells and subjected to RT-PCR. The expression of two splicing variants of *ncRAN* was knocked-down. At the same time, transfected cells were spread onto 24-well plates and the numbers of the cells at indicated time points were counted using hemocytometer and expressed as the mean ± SEM (n=3). *p<0.05. B, Overexpression of *ncRAN* promotes the malignant transformation of NIH3T3 cells. NIH3T3 cells transfected with pcDNA3, pcDNA3-*Nbla10727* and pcDNA3-*Nbla12061* were used to carry out the soft-agar assay as described in Materials and methods. Blank and mock-transfected NIH3T3 cells served as negative controls. #p<0.01.

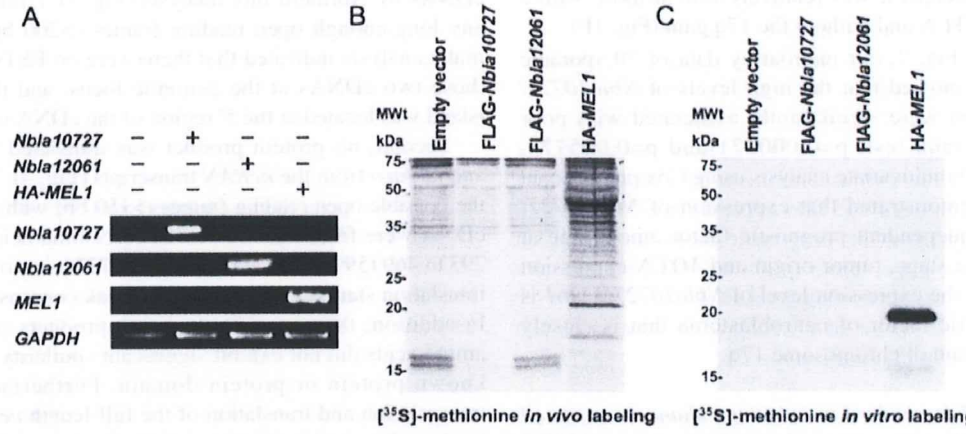

Figure 4. *ncRAN* is a non-protein-coding RNA. A, Ectopic expression of *ncRAN* transcripts in COS7 cells. The *ncRAN* expression vectors were transfected into COS7 cells and total RNA was subjected to RT-PCR. pcDNA3-HA-*MEL1* was used as a positive control. B, *In vivo* [^{35}S]-methionine labeling experiment. COS7 cells transfected with the indicated expression vectors were maintained in fresh growth media without methionine for 2 h and then cultured in the media containing [^{35}S]-methionine overnight. Cells were lysed and subjected to immunoprecipitation with anti-FLAG antibody. Immune complex was washed extensively, resolved by SDS-PAGE and detected by autoradiography. Cell lysate prepared from COS7 cells transfected with pcDNA3-HA-*MEL1* were immunopricipitated with anti-HA antibody. C, *In vitro* translation assay. *In vitro* translation was performed in the presence of [^{35}S]-methionine according to the manufacturer's instructions. pcDNA3-HA-*MEL1* was used as a positive control.

suggest that *ncRAN* might be an evolutionally developed non-coding RNA.

Finally, previous studies have shown that certain large non-coding RNAs are relevant to host RNAs that harbor small RNAs such as microRNA (miRNA) (18). Therefore, we made a search for sequences of known miRNAs in conserved regions within the *ncRAN* locus, but none were identified. These results inferred that the *ncRAN* transcript might not be

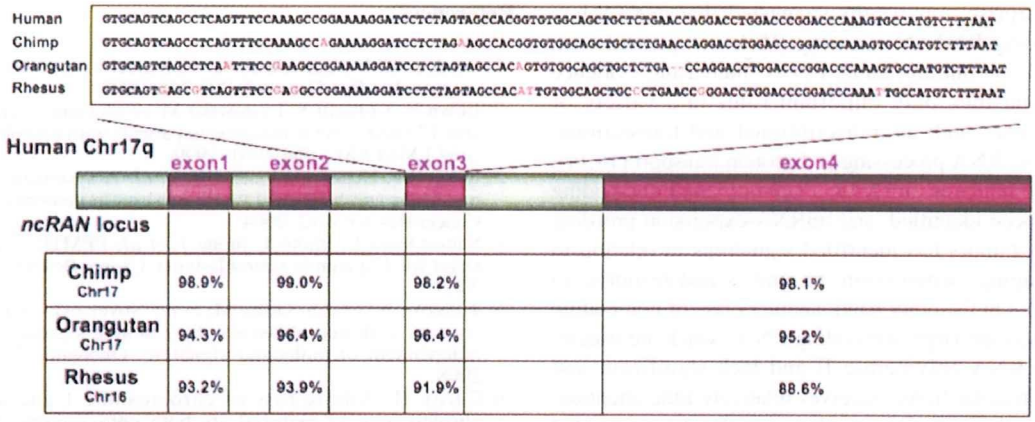

Figure 5. Schematic representation of *ncRAN* sequence conservation in primates. Sequence conservation in *ncRAN* gene locus among human and primates is indicated. Nucleotide sequences of exon3 of *ncRAN* in primates are indicated by numbers in brackets. Genomic sequences within the highly conserved sequence are marked black; mismatches are marked pink. % identities to humans are shown below for each exon. Other lower species, such as mouse, rat, dog, cow, horse, zebrafish, or *C. elegans*, do not have *ncRAN* in their genomes.

Table II. Multivariate analyses of *ncRAN/Nbla10727* mRNA expression as well as other prognostic factors in primary neuroblastomas.

Factor	n	p-value	q-value	H.R.	C.I.
Age (>12-month vs. <12-month)	45 vs. 25	0.0096		3.4	(1.2-9.9)
ncRAN expression	n=70	0.0015	0.0281	3.6	(1.7-7.9)
Age (>18-month vs. <18-month)	40 vs. 30	0.0150		2.9	(1.2-7.1)
ncRAN expression	n=70	0.0023	0.0361	3.5	(1.6-7.8)
Stage (1, 2, 4s vs. 3, 4)	42 vs. 28	<0.0001		8.0	(2.9-14)
ncRAN expression	n=70	0.0457	0.3151	2.4	(1.0-5.6)
Origin (adrenal vs. non-adrenal)	27 vs. 43	<0.0001		9.1	(2.6-33)
ncRAN expression	n=70	0.0107	0.1335	2.8	(1.3-6.1)
MYCN expression	n=70	0.0003		2.0	(1.4-2.8)
ncRAN expression	n=70	0.0035	0.0470	3.3	(1.5-7.3)

n, number of samples; H.R., hazard ratio; C.I., confidence interval. The q-value denotes estimated false discovery rate if all genes whose p-values are equal to or smaller than that of *ncRAN* are discovered as significant (17).

processed to one or more small RNAs. In addition, database search did not identify genes with anti-direction to *ncRAN*, excluding the possibility that *ncRAN* is an antisense gene for certain known genes. Collectively, these results strongly suggested that the *ncRAN* transcript functions as a novel large non-coding RNA.

Discussion

In the present study, we used the combination of array-CGH (5) and gene expression profiling by using an in-house neuroblastoma-proper cDNA microarray (10) to identify genes that strongly correlate with chromosome 17q gain in aggressive neuroblastoma. Our array CGH analysis demonstrated three major genomic groups of chromosomal aberrations such as silent (GGS), partial gains and/or losses (GGP), and whole gains and/or losses (GGW). Correlation analysis revealed that the global feature of the aberrations was maximally correlated with the gain of the long arm of chromosome 17 and with the gain of a whole chromosome 17, therefore the genomic groups GGP and GGW were defined by the status of aberration, by 17q gain and 17 whole chromosomal gain occurred in chromosome 17, respectively (5). Survival analysis for each genetic group suggested that 17q gain was a characteristic and prognosis-related event in primary neuroblastomas. Therefore, we searched for genes that were expressed significantly higher in primary neuroblastomas of GGP compared to that of GGS and GGW and finally found a novel gene *ncRAN* mapped on 17q25.1. The level of its mRNA expression was strongly correlated with the status of chromosome 17 (Table I and Fig. 1B) as well as with patient survival (Table II and Fig. 2).

To our surprise, our results suggested that *ncRAN* is a large non-coding RNA. Non-coding RNA is a general term for functional and untranslatable RNAs. Increasing evidence has shown that they play important roles in a variety of biological events such as transcriptional and translational gene regulation, RNA processing and protein transport (18,19). Recently, the numerous miRNAs, a class of small non-coding RNAs, have been identified, and miRNA-expression profiling of the human tumors has identified signatures in relation to diagnosis, staging, progression, prognosis and response to treatment (19). On the other hand, another class of non-coding RNAs named as the large non-coding RNA, which are usually produced by RNA polymerase II and lack significant and utilized open reading frame, receives relatively little attention. However, recently, increasing number of studies have provided evidence that large non-coding RNAs also play important roles in certain biological processes of the cancers, such as acquisition of drug resistance, transformation, promoting metastasis and inhibition of tumor development (19). In addition, certain candidate non-coding RNAs were isolated from the tissue- and stage-specific libraries, suggesting a possible involvement of non-coding RNAs in development and tumor cell differentiation (20). Given that *ncRAN* was identified from the cDNA libraries generated from different subsets of primary neuroblastomas, it is possible that *ncRAN* might be involved in carcinogenic processes as well as development and differentiation of normal neurons.

In conclusion, we identified a novel large non-coding RNA transcript, *ncRAN*, mapped to the region of 17q gain frequently observed in aggressive neuroblastomas. The levels of *ncRAN* expression are relatively low in normal nerve tissues including adrenal gland, whereas they are upregulated in advanced neuroblastomas with gain of chromosome 17q. From our functional analyses, *ncRAN* appears to act like an oncogene. Notably, knockdown of *ncRAN* with siRNA was able to significantly repress the cell growth in SH-SY5Y neuroblastoma cells with 17q gain as well as high endogenous level of *ncRAN*. Considering emerging evidence on the large non-coding RNAs regulating transcription of other genes (19), the present results not only contribute to further understanding of the molecular and biological mechanism of neuroblastoma genesis, but also provide a potential target for new diagnostic and therapeutic intervention in the future.

Acknowledgements

We are grateful to the hospitals and institutions that provided us with surgical specimens. We also thank Atsushi Kawasaki, Osamu Shimozato, Youquan Bu, Yusuke Suenaga for their valuable suggestions; Shin Ishii for help with microarray statistical analyses; Takehiko Kamijo for providing a *MEL1* plasmid construct; Chengguo Yu for critical reading of the manuscript and Natsue Kitabayashi, Yuki Nakamura, Akane Sada for their technical assistances. This work was supported by Grants-in-Aid for Scientific Research on Priority Areas from the Ministry of Education, Culture, Sports, Science and Technology of Japan and by a Grant-in-Aid from the Ministry of Health, Labour and Welfare of Japan for the Third-Term Comprehensive Control Research for Cancer.

References

1. Brodeur GM: Neuroblastoma: biological insights into a clinical enigma. Nat Rev Cancer 3: 203-216, 2003.
2. Bown N, Cotterill S, Lastowska M, *et al*: Gain of chromosome arm 17q and adverse outcome in patients with neuroblastoma. N Engl J Med 340: 1954-1961, 1999.
3. Riley RD, Heney D, Jones DR, *et al*: A systematic review of molecular and biological tumor markers in neuroblastoma. Clin Cancer Res 10: 4-12, 2004.
4. Saito-Ohara F, Imoto I, Inoue J, *et al*: PPM1D is a potential target for 17q gain in neuroblastoma. Cancer Res 63: 1876-1883, 2003.
5. Tomioka N, Oba S, Ohira M, *et al*: Novel risk stratification of patients with neuroblastoma by genomic signature, which is independent of molecular signature. Oncogene 27: 441-449, 2008.
6. Caron H: Allelic loss of chromosome 1 and additional chromosome 17 material are both unfavourable prognostic markers in neuroblastoma. Med Pediatr Oncol 24: 215-221, 1995.
7. Plantaz D, Mohapatra G, Matthay KK, *et al*: Gain of chromosome 17 is the most frequent abnormality detected in neuroblastoma by comparative genomic hybridization. Am J Pathol 150: 81-89, 1997.
8. Islam A, Kageyama H, Takada N, *et al*: High expression of Survivin, mapped to 17q25, is significantly associated with poor prognostic factors and promotes cell survival in human neuroblastoma. Oncogene 19: 617-623, 2000.
9. Ohira M, Oba S, Nakamura Y, *et al*: A review of DNA microarray analysis of human neuroblastomas. Cancer Lett 228: 5-11, 2005.
10. Ohira M, Oba S, Nakamura Y, *et al*: Expression profiling using a tumor-specific cDNA microarray predicts the prognosis of intermediate risk neuroblastomas. Cancer Cell 7: 337-350, 2005.
11. Brodeur GM, Pritchard J, Berthold F, *et al*: Revisions of the international criteria for neuroblastoma diagnosis, staging and response to treatment. J Clin Oncol 11: 1466-1477, 1993.
12. Kaneko M, Tsuchida Y, Mugishima H, *et al*: Intensified chemotherapy increases the survival rates in patients with stage 4 neuroblastoma with MYCN amplification. J Pediatr Hematol Oncol 24: 613-621, 2002.
13. Iehara T, Hosoi H, Akazawa K, *et al*: MYCN gene amplification is a powerful prognostic factor even in infantile neuroblastoma detected by mass screening. Br J Cancer 94: 1510-1515, 2006.
14. Suzuki Y, Yoshitoma-Nakagawa K, Maruyama K, *et al*: Construction and characterization of a full length-enriched and a 5'-end-enriched cDNA library. Gene 200: 149-156, 1997.
15. Ohira M, Morohashi A, Nakamura Y, *et al*: Neuroblastoma oligo-capping cDNA project: toward the understanding of the genesis and biology of neuroblastoma. Cancer Lett 197: 63-68, 2003.
16. Ohira M, Morohashi A, Inuzuka H, *et al*: Expression profiling and characterization of 4200 genes cloned from primary neuroblastomas: identification of 305 genes differentially expressed between favorable and unfavorable subsets. Oncogene 22: 5525-5536, 2003.
17. Storey JD and Tibshirani R: Statistical significance for genome-wide studies. Proc Natl Acad Sci USA 100: 9440-9445, 2003.
18. Mattick JS and Makunin IV: Non-coding RNA. Hum Mol Genet 15: R17-R19, 2006.
19. Prasanth KV and Spector DL: Eukaryotic regulatory RNAs: an answer to the 'genome complexity' conundrum. Genes Dev 21: 11-42, 2007.
20. Numata K, Kanai A, Saito R, *et al*: Identification of putative noncoding RNAs among the RIKEN mouse full-length cDNA collection. Genome Res 13: 1301-1306, 2003.

Oncogene (2010), 1–10

www.nature.com/onc

ORIGINAL ARTICLE

Bmi1 is a MYCN target gene that regulates tumorigenesis through repression of *KIF1Bβ* and *TSLC1* in neuroblastoma

H Ochiai[1,2], H Takenobu[1], A Nakagawa[3], Y Yamaguchi[1], M Kimura[1], M Ohira[4], Y Okimoto[5], Y Fujimura[6], H Koseki[6], Y Kohno[2], A Nakagawara[7] and T Kamijo[1]

[1]Division of Biochemistry and Molecular Carcinogenesis, Chiba Cancer Center Research Institute, Chiba, Japan; [2]Department of Pediatrics, Graduate School of Medicine, Chiba University, Chiba, Japan; [3]Department of Pathology, National Center for Child Health and Development, Tokyo, Japan; [4]Laboratory of Cancer Genomics, Chiba Cancer Center Research Institute, Chiba, Japan; [5]Department of Hematology and Oncology, Chiba Children's Hospital, Chiba, Japan; [6]Developmental Genetics Group, RIKEN Research Center for Allergy and Immunology, Yokohama, Japan and [7]Division of Innovative Cancer Therapeutics, Chiba Cancer Center Research Institute, Chiba, Japan

Recent advances in neuroblastoma (NB) research addressed that epigenetic alterations such as hypermethylation of promoter sequences, with consequent silencing of tumor-suppressor genes, can have significant roles in the tumorigenesis of NB. However, the exact role of epigenetic alterations, except for DNA hypermethylation, remains to be elucidated in NB research. In this paper, we clarified the direct binding of MYCN to Bmi1 promoter and upregulation of Bmi1 transcription by MYCN. Mutation introduction into an MYCN binding site in the Bmi1 promoter suggests that MYCN has more important roles in the transcription of Bmi1 than E2F-related Bmi1 regulation. A correlation between MYCN and polycomb protein Bmi1 expression was observed in primary NB tumors. Expression of Bmi1 resulted in the acceleration of proliferation and colony formation in NB cells. Bmi1-related inhibition of NB cell differentiation was confirmed by neurite extension assay and analysis of differentiation marker molecules. Intriguingly, the above-mentioned Bmi1-related regulation of the NB cell phenotype seems not to be mediated only by p14ARF/p16INK4a in NB cells. Expression profiling analysis using a tumor-specific cDNA microarray addressed the Bmi1-dependent repression of *KIF1Bβ* and *TSLC1*, which have important roles in predicting the prognosis of NB. Chromatin immunoprecipitation assay showed that *KIF1Bβ* and *TSLC1* are direct targets of Bmi1 in NB cells. These findings suggest that MYCN induces Bmi1 expression, resulting in the repression of tumor suppressors through Polycomb group gene-mediated epigenetic chromosome modification. NB cell proliferation and differentiation seem to be partially dependent on the MYCN/Bmi1/tumor-suppressor pathways.
Oncogene advance online publication, 1 March 2010; doi:10.1038/onc.2010.22

Correspondence: Professor T Kamijo, Division of Biochemistry and Molecular Carcinogenesis, Chiba Cancer Center Research Institute, 666-2 Nitona, Chuo-ku, Chiba 260-8717, Japan.
E-mail: tkamijo@chiba-cc.jp
Received 27 August 2009; revised 19 November 2009; accepted 4 January 2010

Keywords: Bmi1; MYCN; neuroblastoma; TSLC1; KIF1Bβ

Introduction

In tumorigenesis, besides the well-known genetic changes that occur in cancer, such as the deletion of tumor-suppressor genes (TSGs), amplification/activation of oncogenes and loss of heterozygosity or gene mutations in tumor-associated genes (Hanahan and Weinberg, 2000), epigenetic alterations, such as altered DNA methylation, misregulation of chromatin remodeling by histone modifications and aberrant expression of Polycomb group genes (PcGs) proteins have emerged as common hallmarks of many cancers (Jones and Baylin, 2002; Sparmann and van Lohuizen, 2006; Esteller, 2007; Rajasekhar and Begemann, 2007). PcGs are usually considered to be transcriptional repressors that are required for maintaining the correct spatial and temporal expressions of homeotic genes during development. (Schwartz and Pirrotta, 2008). Recent biochemical approaches have established that PcG proteins form multiprotein complexes, known as Polycomb-Repressive Complexes (PRCs). PRC2 contain Ezh2, EED, Suz12 and RbAp48, whereas the PRC1 complex consists of >10 subunits, including the oncoprotein Bmi1 and the HPC proteins, namely HPH1-3, RING1-2 and SCML (Rajasekhar and Begemann, 2007). In addition to being essential regulators of embryonic development, PcGs have also emerged as key players in the maintenance of adult stem cell populations (Valk-Lingbeek *et al.*, 2004; Pietersen and van Lohuizen, 2008). For example, Bmi1 is required for the self-renewal of hematopoietic and neural stem cells (Lessard and Sauvageau, 2003; Molofsky *et al.*, 2003, Iwama *et al.*, 2004), whereas the overexpression of EZH2 prevents hematopoietic stem cell exhaustion (Kamminga *et al.*, 2005). Consistent with their critical roles in development, differentiation and stem cell renewal, several PcGs are oncogenes, overexpressed in both solid and hematopoietic cancers (Valk-Lingbeek *et al.*, 2004; Rajasekhar and Begemann, 2007).

Neuroblastoma (NB) is one of the most common malignant solid tumors occurring in infancy and childhood and accounts for 10% of all pediatric cancers (Westemann and Schwab, 2002). NBs are derived from sympathetic neuroblasts with various clinical outcomes from spontaneous regression, caused by neuronal differentiation and/or apoptotic cell death, to malignant progression. Extensive cytogenetic and molecular genetic studies identified that genetic abnormalities, such as loss of the short arm of chromosome 1 (1p), amplification of *MYCN* and 17q gain, are frequently observed and often associated with poor clinical outcome (Brodeur *et al.*, 1984; Caron, 1995). Although numerous genetic abnormalities, including *MYCN* amplification, are involved in the development and/or progression of NB, the molecular mechanisms responsible for the pathogenesis of aggressive NB remain unclear. Epigenetic alterations, such as hypermethylation of promoter sequences, with consequent silencing of TSGs, such as *CASP8*, *RASSF1A*, *CD44*, *TSP-1* and *PTGER2*, can have significant roles in the tumorigenesis of NB (Teitz *et al.*, 2000; Yan *et al.*, 2003; Yang *et al.*, 2003, 2004; Sugino *et al.*, 2007). However, it was reported that the expression of several tumor-suppressor candidate genes, such as KIF1Bβ and TSLC1, is suppressed in NB cells, but the percentage of pathological mutations and promoter methylation in NB tumors was not so high (Ando *et al.*, 2008; Munirajan *et al.*, 2008). For the promoter DNA methylation-independent gene repression, the PcG complex might have a role in NB cell proliferation and differentiation, although the exact role of PcG in NB tumorigenesis remains to be elucidated. Regarding Bmi1 regulation in NB, the binding of E2F-1 to Bmi1 promoter and its activation were reported, and a strong expression of Bmi1 was observed in primary NBs (Nowak *et al.*, 2006). However, Bmi1 expression was not evaluated according to patient prognosis, and there was no correlation between *MYCN* amplification and Bmi1 expression in the report. Another group reported that Bmi1 suppression by knockdown induced several differentiation marker proteins, and impaired colony formation and tumor formation in immunodeficient mice, although Bmi1 overexpression in NB cells could not function as an oncogene (Cui *et al.*, 2006, 2007).

In this paper, we found that MYCN directly bound to Bmi1 promoter and induced its transcription. A correlation between MYCN and Bmi1 expressions was observed in both NB cell lines and primary tumors. The expression of Bmi1 in NB cells resulted in the upregulation of proliferation and colony formation; expression profiling using a tumor-specific cDNA microarray (Ohira *et al.*, 2005) addressed the Bmi1-dependent repression of TSGs, which has an important role in predicting the prognosis of NB.

Results

Bmi1 expression correlates with MYCN expression in NB cell lines and tumor samples

First, we studied Bmi1 expression by western blotting and found that the PRC1 complex protein Bmi1 and Ring1b expressions correlated with MYCN protein expression in NB cell lines, except for SK-N-AS cells (Figure 1Aa). At the mRNA level, we observed Bmi1 upregulation in *MYCN*-amplified SK-N-DZ to IMR32 cells (Figure 1Ab). Furthermore, the Bmi1 expression in primary NB specimens was clearly detected in the nucleus of *MYCN*-amplified NBs compared with those of *MYCN* single-copy NBs (Supplementary Figure S1), which was confirmed by statistical analysis (Figure 1B).

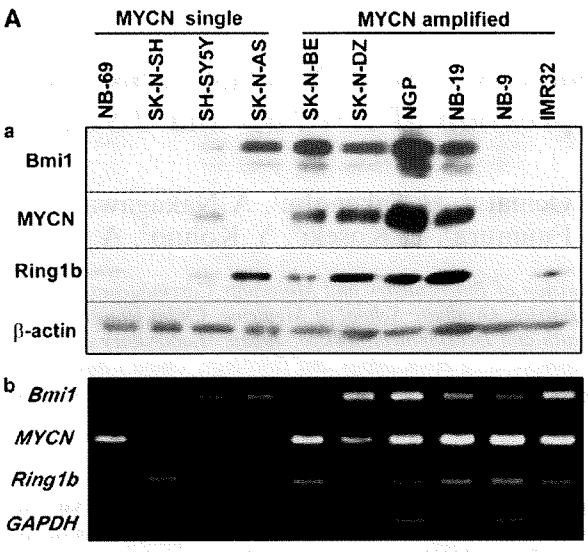

B

MYCN	Bmi1 Nuc (+)	Bmi1 Nuc (-)
single	0	10
amplified	5	1

Fisher's exact probability test
P<0.01

Figure 1 Bmi1 expression correlates with MYCN in NB (**A**). Bmi1 expression in NB cell lines. Western blotting analysis (a) and semi-quantitative RT–PCR (b) of Bmi1, Ring1b and MYCN were performed as described in the 'Materials and methods' section. (**B**) Immunohistochemical analysis of Bmi1 in NB tumor samples. In all, 10 *MYCN* single-copy NBs and 6 amplified NBs were analyzed. Statistical significance was determined by Fisher's exact probability test.

Bmi1 transcription is induced by MYCN

The above findings prompted us to study whether Bmi1 transcription is induced by MYCN in NB cells. We used Tet21/N cells expressing MYCN under the control of tetracycline (Lutz *et al.*, 1996). Four hours after tetracycline withdrawal, Bmi1 and Ring1b expressions were considerably increased along with MYCN induction both at mRNA and protein levels (Figure 2A a,b) associated with MYCN induction.

Using *in silico* analysis by the TFSEARCH program (http://www.cbrc.jp/research/db/TFSEARCHJ.html), we identified an MYCN binding site (E-box) at positions −181 and −764, −319 and −122 E2F binding

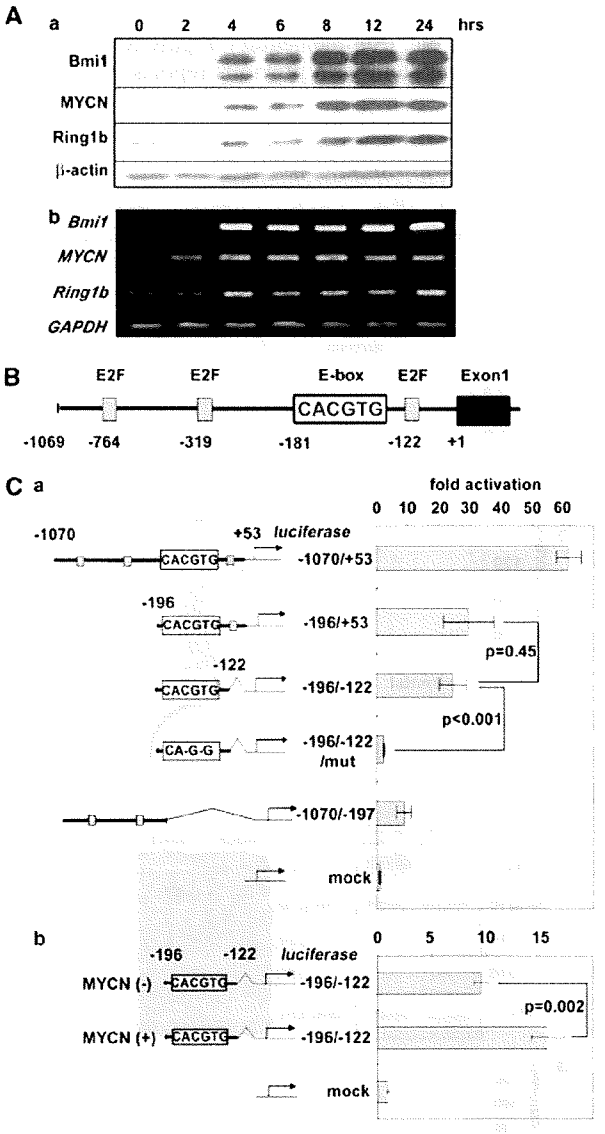

Figure 2 Bmi1 transcription is induced by MYCN. (**A**) Bmi1 expression was studied in MYCN-inducible Tet21/N cells. After withdrawal of tetracycline from culture medium, cells were collected at the indicated time points and analyzed by western blotting (Aa) and semi-quantitative RT–PCR (Ab). (**B**) Human Bmi1 promoter showing the locations (E2F sites and putative MYCN binding E-box) and sequence (putative MYCN binding E-box). Position +1 means the 5′ end of the RefSeq cDNA sequence (NM_005180). (**C**) MYCN activates Bmi1 through the binding site in the promoter. SK-N-DZ (*MYCN* amplified) and Tet21/N (MYCN-inducible) NB cells were transiently cotransfected with the indicated Bmi1 promoter-controlled reporter constructs. E2F site 1 and site 2 were deleted in the −196/+53 fragment; E2F sites 1–3 were deleted in the −196/−122 fragment. The results are representative of at least three independent experiments. Error bars represent the s.d. obtained with triplicate samples. Statistical significance was determined by the Mann–Whitney test.

sites in the human Bmi1 promoter (ENSG00000168283) (Figure 2B). To study the transcriptional regulation of Bmi1 expression in NB cells, initial transfection experiments were conducted with the Bmi1 luciferase/promoter reporter construct (−1070/+53), which contains the putative E-box element and E2F binding sites (Figure 2Ca); the −1070/+53 fragment showed significant promoter activity in an *MYCN*-amplified NB cell line SK-N-DZ. Deletion of −1070/−197 and −121/+53 still showed considerable activity (Figure 2Ca, activity of −196/+53 fragment compared with −196/−122), suggesting an important role of MYCN in Bmi1 promoter activity. Furthermore, this finding was confirmed by mutation of the E-box in the −196/−122 fragment (activity of −196/−122/mut).

Next, we studied the effect of MYCN on Bmi1 promoter activity using the MYCN-inducing NB cell line Tet21/N. MYCN induction significantly increased promoter activity in Tet21/N cells (Figure 2Cb). Intriguingly, we observed promoter activity even in MYCN (−) cells. We speculated that residual MYC (c-MYC) may contribute to activity in these cells (Supplementary Figure S2)

MYCN binds to the E-box region in Bmi1 promoter

To address whether MYCN could be recruited onto the E-box in Bmi1 promoter in NB cells, we performed chromatin immunoprecipitation (ChIP) assays by quantitative real-time PCR (qPCR). We found that MYCN binding to the Bmi1 promoter region was clearly detected in *MYCN*-amplified SK-N-DZ and NB-19 cells but not in *MYCN*-single SH-SY5Y cells (Figure 3a). Furthermore, this observation was confirmed in MYCN-inducible Tet21/N cells (Figure 3b), indicating that MYCN binds to the Bmi1 promoter region and has a considerable role in Bmi1 transcription in *MYCN*-amplified NB tumors.

Bmi1 regulates NB cell proliferation

Next, we examined the effect of Bmi1 on the cell growth of NB cells by exogenous expression of Bmi1. SH-SY5Y cells were infected with the mock virus and the FLAG-tagged Bmi1 expression virus. Cell growth was studied by the WST (water-soluble tetrazolium salt) assay and showed that Bmi1 significantly accelerated cell proliferation compared with mock cells (Figure 4a). In the soft agar assay, Bmi1-expressing SH-SY5Y cells formed anchorage-independent colonies effectively, although colony formation was hardly detectable in parental and mock cells (Figure 4b). Interestingly, Ring1b was increased in Bmi1-expressing SH-SY5Y cells (Figure 4c) and Tet21/N cells (Figure 4e); the well-known Bmi1 targets p14ARF and p16INK4a protein amounts were not markedly changed by Bmi1 expression, although mRNA expression was slightly suppressed in SH-SY5Y cells. These results suggest that increased PRC1-mediated gene repression, except for p14ARF and p16INK4a, might have an important role in NB cells. In addition, we found an additive effect of MYCN induction in Bmi1-expressing Tet21/N cells, suggesting the significance of MYCN targets, except for Bmi1, in NB cell proliferation. Bmi1 knockdown by lentivirus-mediated shRNA transduction strongly inhibited cell

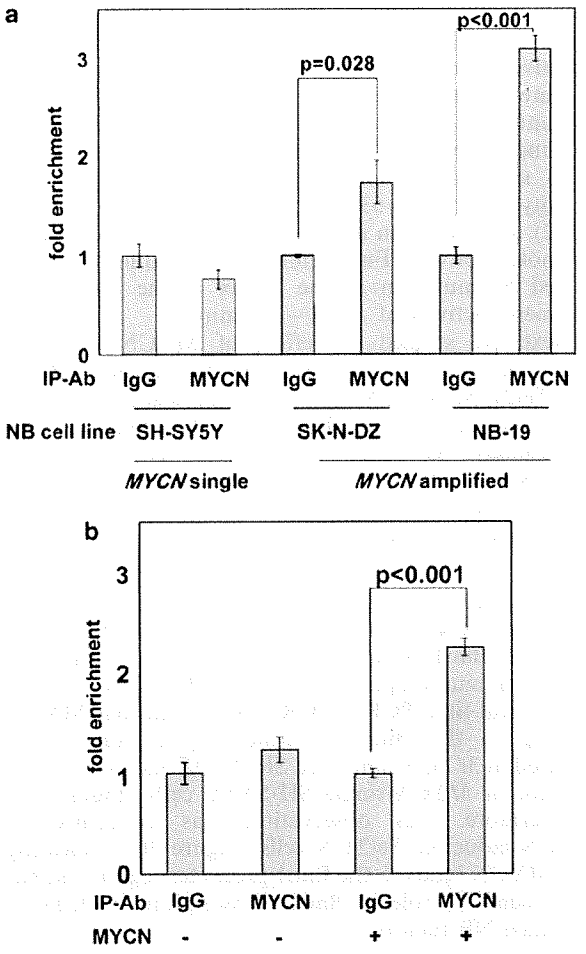

Figure 3 MYCN binds to human Bmi1 promoter *in vivo*. Cross-linked chromatin was isolated from SH-SY5Y (*MYCN* single copy, a), SK-N-DZ and NB-19 (*MYCN* amplified, panel a) and Tet21/N (MYCN-inducible, b) NB cells. Immunoprecipitation was performed with an anti-MYCN antibody (clone NCM II 100) or control IgG. The precipitated chromatin was used as templates for qPCR analysis as described in the 'Materials and methods' section. In panel b experiments, Tet21/N were cultured in the condition of either tet-off (MYCN (+)) or tet-on (MYCN (−)). The results are representative of at least three independent experiments. Error bars represent the s.d. obtained with triplicate samples. Statistical significance was determined by the Mann–Whitney test.

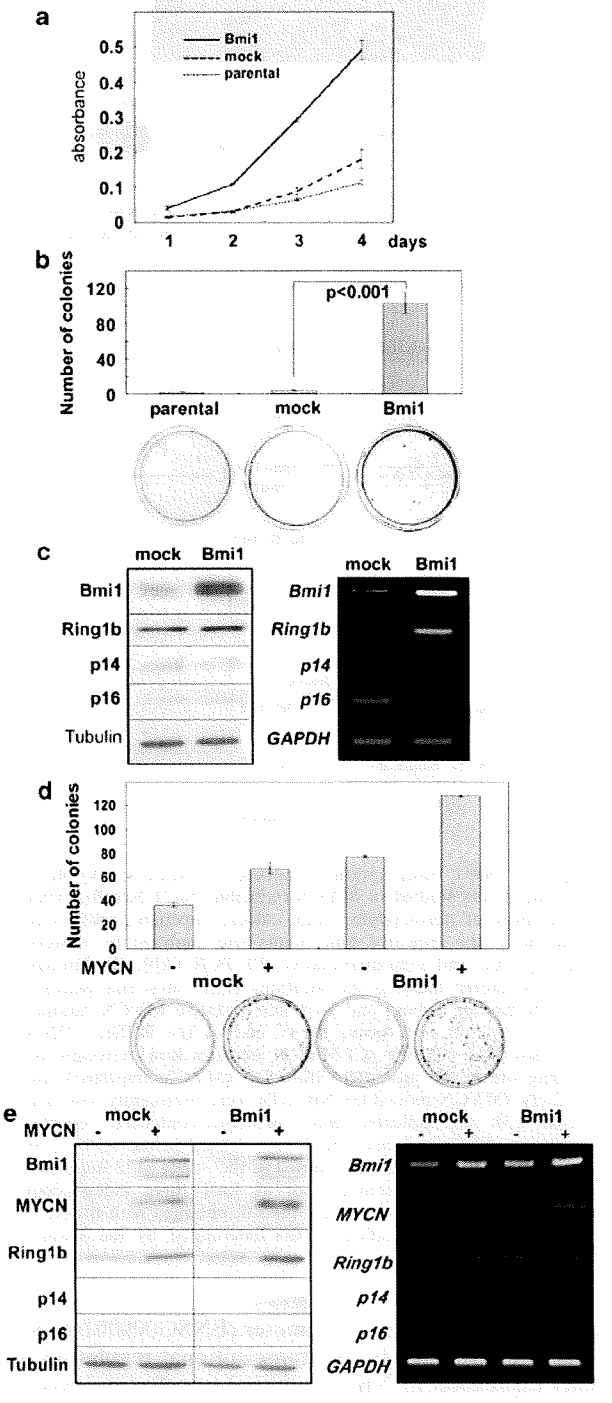

Figure 4 Bmi1 effects on NB cell proliferation. WST assay (a) and soft agar colony formation assay (b) of Bmi1-expressing NB cells (SH-SY5Y). The results are representative of at least three independent experiments. Error bars represent the s.d. obtained with triplicate samples. (c) Western blotting (left panel) and semi-quantitative RT–PCR assay (right panel) of Bmi1-expressing SH-SY5Y cells. Analyzed molecules are shown in the left margin of the panels. (d) Soft agar colony formation assay of Bmi1-expressing NB cells (Tet21/N). Tet21/N cells were infected with either mock lentivirus (Bmi1 (−)) or Bmi1-expressing lentivirus (Bmi1 (+)), and cultured with either Tet(−) (MYCN+) or Tet(+) (MYCN−) complete soft agar media. The results are representative of at least three independent experiments. Error bars represent the s.d. obtained with triplicate samples. Statistical significance was determined by the Mann–Whitney test. (e) Western blotting (left panel) and semi-quantitative RT-PCR assay (right panel) of Tet21/N cells treated as described above. Analyzed molecules are shown in the left margin of the panels.

proliferation in several NB cell lines, such as SK-N-AS, IMR32, TGW, etc. (Supplementary Figure S3 and data not shown), consistent with previous reports (Cui *et al.*, 2006).

Bmi1 controls NB cell differentiation

Treatment with TPA (12-*O*-tetradecanoylphorbol 13-acetate) or ATRA (all-trans-retinoic acid) effectively

induced NB cell differentiation, for example, neurite extension (Figure 5Aa), and the expression of differentiation markers (Figure 5Ab and c). Interestingly, Bmi1 was downregulated at the protein level along with NB cell differentiation by TPA or ATRA treatment. To address the role of Bmi1 in NB cell differentiation, we knocked down Bmi1 using shRNA-expressing lentivirus. Intriguingly, only Bmi1 knockdown induced significant neurite extension (Figure 5Ba) and the expression of differentiation markers GAP43 and NF68 (Figure 5Bc), suggesting the existence of Bmi1-related regulation of NB cell differentiation.

Bmi1 binds to the promoter region of TSGs TSLC1 and KIF1Bβ and suppresses transcription in NB cells

To understand how Bmi1 controls NB cell proliferation and tumorigenesis, we chose to identify their target genes, except for p14ARF/p16INK4a, as we could not observe significant changes in these well-known tumor suppressors (Figures 4 and 5). To identify the Bmi1 target genes, except for p14ARF and p16INK4a, we studied expression gene profiling using an appropriate NB cDNA microarray (named the CCC-NHR13000 chip) carrying 13 440 cDNA spots. The top 10 genes decreased by Bmi1 expression in SK-N-BE cells are listed in Table 1. Surprisingly, the well-known tumor suppressors (TSGs) in NB TSLC1 (NM_014333.3) and KIF1Bβ (AB017133) are ranked as the first and second targets, respectively. The previously reported Bmi1 target HOXA4 expression (Cao *et al.*, 2005) was also considerably repressed by Bmi1. Consistent with our results (Figures 4 and 5), the ranking of p14ARF/p16INK4a was 5258. We determined the Bmi1-mediated regulation of *TSLC1* and *KIF1Bβ* transcription by semi-quantitative real-time (RT)-PCR experiments using Bmi1-expressing and knocked-down NB cells and found that Bmi1 expression considerably repressed *TSLC1* and *KIF1Bβ* transcription in NB cells (Figure 6a). Next, we studied Bmi1 binding to the promoter regions of *TSLC1* and *KIF1Bβ* and found that Bmi1 specifically bound to the KIF1Bβ (ENSG00000054523) and TSLC1 (ENSG00000105767) promoter region in NB cells. qPCR ChIP expressions confirmed Bmi1 binding to these promoters, suggesting the existence of MYCN/Bmi1-mediated *TSLC1* and *KIF1Bβ* suppression in NB. Furthermore, this Bmi1-mediated regulation of *TSLC1* and *KIF1Bβ* expression was not only in NB cells but also in squamous lung cancer QG56 cells (Supplementary Figure S4).

Discussion

Bmi1 regulates the expression of TSGs in NB

Among the PcG target genes in cancer cells, PcG-mediated repression of TSGs has an indispensable role in tumorigenesis (Sparmann and van Lohuizen, 2006; Rajasekhar and Begemann, 2007). As a result of PcG overexpression, the increased PRC1/PRC2 complexes bind to PcG target gene promoter lesions. Next, putative

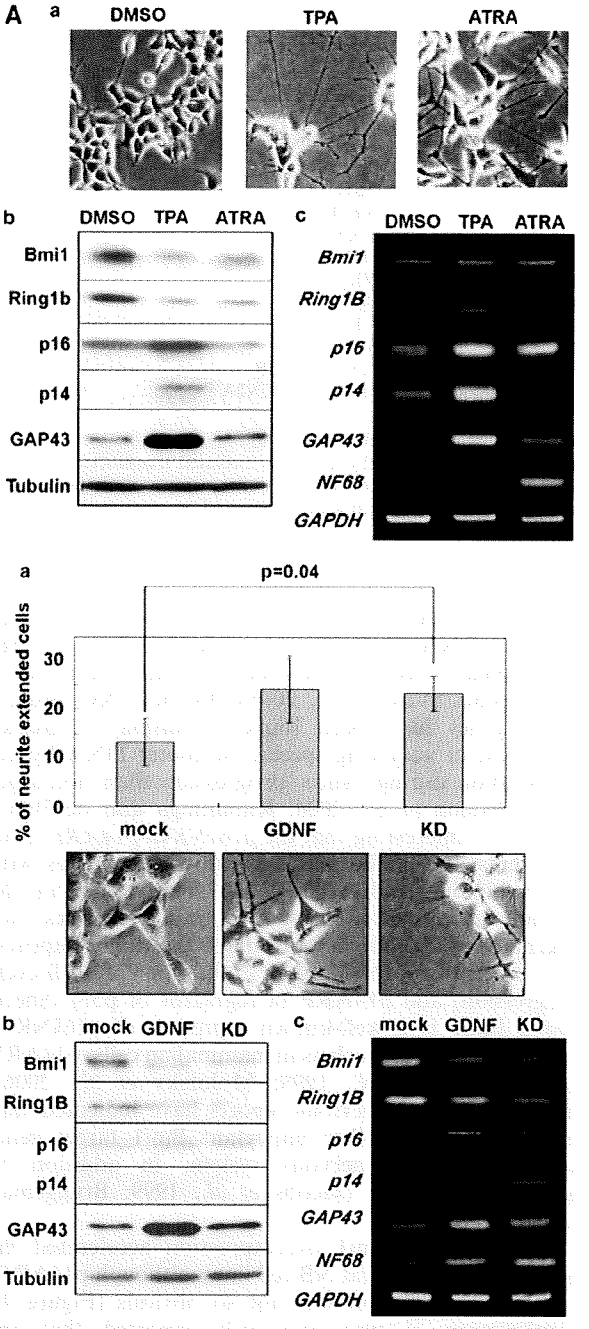

Figure 5 Bmi1 regulates NB cell differentiation. (**A**) TGW cells were treated with 0.1% DMSO, 100 nM of 12-*O*-tetradecanoylphorbol-13-acetate (TPA) and 5 μM all-trans-retinoic acid (RA) for 72 h. Neurite extension (a) was analyzed as described in the 'Materials and methods' section, and the indicated molecule expression was studied by western blotting analysis (b) and semi-quantitative RT–PCR assay (c). (**B**) TGW cells were infected with either mock- or Bmi1-knockdown lentivirus, as described in the 'Materials and methods' section. Neurite extension was assayed using mock-infected (left), mock-infected 10 ng/ml GDNF (middle) and Bmi1-knocked down (right) TGW cells. The results are representative of at least three independent experiments. Error bars represent the s.d. obtained with triplicate samples. Statistical significance was determined by the Mann–Whitney test. We could not detect NF68 expression at the protein level.

Table 1 Top 10 genes suppressed by Bmi1 in NB cells

Rank	*Gene name*	*Symbol*	*Accession*	*Fold induction (log(Bmi1)/log(GFP))*
1	KIF1B	KIF1B	AB011163	−2.961
2	TSLC1	TSLC1	NM_014333	−1.469
3	CHGA	CHGA	NM_001275	−1.296
4	DBH	DBH	NM_000787	−1.263
5	WKID22370	ARCN1	NM_001655	−1.206
6	WKID02790	KIAA0970	NM_014949	−1.184
7	FHL1	FHL1	NM_001449	−1.167
8	WKID21762	TMP21	NM_006827	−1.121
9	Nbla20566	RISC	NM_021626	−1.105
10	WKID00168	ENO1	NM_001428	−1.097
757	HOXA4	HOXA4	NM_002141	−0.439
1528	P15_CDKN2B	CDKN2B	NM_004936	−0.314
5258	P16_P14CDKN2A	CDKN2A	NM_000077	−0.009

Abbreviation: NB, neuroblastoma.
Bmi1 was overexpressed by lentivirus-mediated transduction in SK-N-BE cells. Total RNA was extracted and subjected to expression profiling analysis by an appropriate NB cDNA microarray as described in the 'Materials and methods' section. The results are the averages of at least three experiments and the top 10 genes suppressed are presented. Overall, 11 293 genes were analyzed. We will inform the microarray data if there is a request.

PRC/DNA methyltransferase cross talk seems to induce aberrant DNA methylation as PRC2 member EZH2 was shown to recruit DNA methyltransferase to select target genes (Viré *et al.*, 2006). In fact, PcG protein target genes have been found to display a greater likelihood of acquiring specific promoter DNA hypermethylation during cancer progression than nontarget genes (Iwama *et al.*, 2004; Kamminga and de Haan, 2006). It is interesting that the *p16INK4a-p14ARF* locus represents one of the above-identified candidates with PRCs binding and hyper DNA methylation in the promoters in cancer cells. This locus encodes two alternatively spliced gene products, the tumor-suppressor protein p16INK4a (an inhibitor of cell-cycle progression) and p14ARF (a regulator of p53) (Sherr, 2004). Bmi1 is a well-known repressor of p16INK4a and, in some cases, such as in mammalian cells, p14ARF genes (Jacobs *et al.*, 1999; Molofsky *et al.*, 2006). However, several previous reports have indicated that there could be another important Bmi1 target gene, especially in the nervous system, in addition to p16INK4a/p14ARF (Jacobs *et al.*, 1999; Bruggeman *et al.*, 2007).

In our study, Bmi1 overexpression accelerated the proliferation of several NB cell lines, although p14ARF/p16INK4a repression was not so obvious (Figure 4). Furthermore, it was previously reported that the probability of p16INK4a inactivation in NB was not high (Easton *et al.*, 1998). These results prompted us to screen Bmi1-dependent gene repression using a tumor-specific cDNA microarray, and we identified the repression of TSGs, *KIF1Bβ* and *TSLC1* (Table 1). This repression was confirmed by semi-quantitative RT-PCR experiments, and the *in vivo* binding of Bmi1 to these promoters was addressed by ChIP assay with qPCR using Bmi1-overexpressing NB cells (Figure 6). Accumulating lines of evidence strongly suggest that downregulation of TSLC1 in various cancers, including lung cancer, hepatocellular carcinoma, gastric cancer, pancreatic adenocarcinoma, prostate cancer, breast cancer, nasopharyngeal carcinoma and cervical cancer, might be due to the hypermethylation of its promoter region (Murakami, 2005). In sharp contrast to these cancers, we did not detect hypermethylation of the promoter region of the *TSLC1* gene in primary NBs or NB-derived cell lines, and *TSLC1* expression levels significantly correlated with the stage, Shimada's pathological classification and *MYCN* amplification status (Ando *et al.*, 2008). We also found that *KIF1Bβ*, located at chromosome 1p36.2, was significantly suppressed in *MYCN*-amplified NB samples, although its mutation rate was not high and promoter hypermethylation was not observed (Munirajan *et al.*, 2008). Furthermore, a previous report mentioned that a cluster of genes located in 1p36, including *KIF1Bβ*, is downregulated in NBs with poor prognosis, but was not due to CpG island methylation (Carén *et al.*, 2005). Taken together, it suggests that MYCN-induced Bmi1 suppresses several TSGs by their promoter silencing and contributes to NB tumorigenesis. Systematic analysis of PcG binding to gene promoter lesions will be required for the study of epigenetic regulation of tumorigenesis-related gene expression in NB.

Regulation of Bmi1 gene transcription

Despite these important functions in development and tumorigenesis, little is known about transcriptional regulation of the *Bmi1* gene. The transcription factors known to regulate Bmi1 expression are sonic hedgehog-activated Gli1 protein (Leung *et al.*, 2004), E2F family members (Nowak *et al.*, 2006), zinc-finger transcription factor SALL4 (Yang J *et al.*, 2007) and c-Myc (Guney *et al.*, 2006). As E2F1 regulates NB tumorigenesis through direct binding to *MYCN* promoter and its activation, E2F may regulate NB cells using complicated MYCN, MYCN/Bmi1 and Bmi1 regulation mechanisms (Strieder and Lutz, 2003; Kramps *et al.*, 2004).

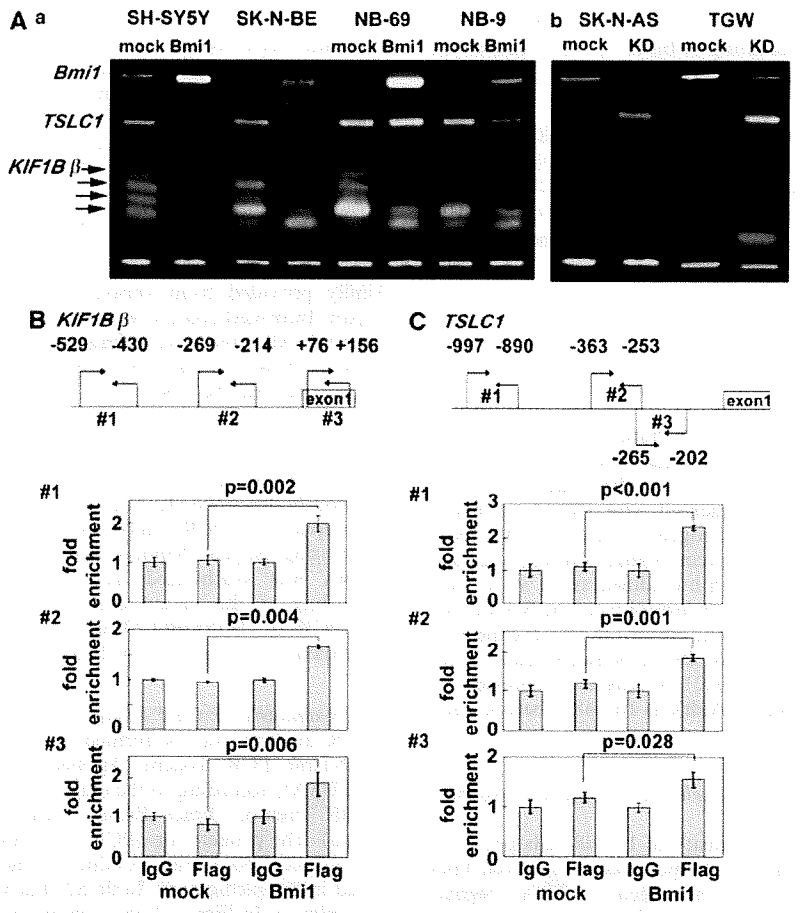

Figure 6 Bmi1 directly binds to TSLC1 and KIF1Bβ promoters and represses transcription in NB cells. (A) The indicated NB cell lines were infected with Bmi1-expressing lentivirus (a) and Bmi1-shRNA lentivirus (b), as described in the 'Materials and methods' section. Bmi1 expression modulated by lentivirus infection was examined (top lane of panels). TSLC1 and KIF1Bβ expressions were studied by semi-quantitative RT–PCR assay. The primer sequences are shown in Supplementary Table S1. The results are representative of at least three independent experiments. Arrows indicate alternative splicing products of KIF1Bβ (Munirajan *et al.*, 2008). (B: KIF1Bβ and C: TSLC1) SK-N-BE cells were infected with FLAG-Bmi1-expressing lentivirus and subjected to quantitative ChIP assay as described in the 'Materials and methods' section. Immunoprecipitation was performed by anti-FLAG (M2) antibody and control mouse IgG. The primers for qPCR analysis were designed using the Primer3 program (Applied Biosystems, Foster City, CA, USA) and locations are indicated in the diagrams. The primer sequences are shown in Supplementary Table S2. The results are presented as fold enrichment and are representative of at least three independent experiments. Error bars represent the s.d. obtained with triplicate samples. Statistical significance was determined by the Mann–Whitney test.

In this paper, we found that MYCN directly binds to the Bmi1 promoter *in vivo* and that binding is enhanced by *MYCN* amplification in NB cell lines and MYCN induction using tetracycline-withdrawal-based gene induction plasmid (Figure 3). MYCN expression correlates with Bmi1 levels both at mRNA and protein levels in NB cell lines (Figures 1A, 2a) and NB tumor samples (Figure 1b). Next, we studied the role of the MYCN binding site and several E2F binding sites in Bmi1 transcriptional regulation using a luciferase expression system (Figure 2). Intriguingly, we found that significantly high luciferase activities of E-box + E2F site promoter (Figure 2c, −196/+53 fragment) and E2F site deletion from this fragment (Figure 2c, −196/−122 fragment) resulted in only a modest reduction of activity. Furthermore, base-deleted mutation to the E-box almost completely suppressed the activity of the deltaE2F fragment (Figure 2c, −196/−122/mut), suggesting the role of MYCN in Bmi1 transcription. MYCN-dependent Bmi1 induction was observed not only in NB cell experiments but also in *in vivo* experiments. The Bmi1 mRNA level was higher in NBs occurring in tyrosine hydroxylase promoter-induced *MYCN* transgenic mice than in ganglions with hyperplasia and normal ganglion (S Kishida and K Kadomatsu, personal communication). Accordingly, these results suggest the important role of MYCN in Bmi1 transcription in NB and further studies will be required to address the exact mechanism of Bmi1 transcriptional regulation by E2F and/or MYCN.

Furthermore, the epigenetic regulation of Bmi1 transcription will be an interesting subject of NB research as we observed considerable effects of Bmi1 on other PRC complex proteins.

Taken together, we found an intriguing MYCN/Bmi1/tumor-suppressor pathway in NB cells. This pathway might have a remarkable impact on NB tumorigenesis and is considered a target for the development of molecular targeted therapy for therapy-resistant NBs.

Materials and methods

Cell culture
Human NB cell lines and QG56 human lung squamous carcinoma cells were obtained from official cell banks and were cultured in RPMI1640 or Dulbecco's modied Eagle's medium (Wako, Osaka, Japan) supplemented with 10% heat-inactivated fetal bovine serum (Invitrogen, Carlsbad, CA, USA) and 50 μg/ml penicillin/streptomycin (Sigma-Aldrich, St Louis, MO, USA) in an incubator with humidified air at 37 °C with 5% CO_2. Tet21/N cells, which are derived from the SH-EP NB cell line, express MYCN under the control of tetracycline (tet-off system) (kindly provided by Dr M Schwab; Lutz *et al.*, 1996). MYCN expression in Tet21/N cells was repressed by 100 ng/ml tetracycline (Sigma-Aldrich) for 48 h before each experiment.

Treatment of cell lines with glial cell line-derived neurotrophic factor, ATRA or TPA
TGW cells were seeded at a density of 1×10^5 cells per 6-cm diameter tissue culture dish in the presence of glial cell line-derived neurotrophic factor (Invitrogen), ATRA (Sigma-Aldrich) or TPA (Nacalai Tesque, Kyoto, Japan) at the concentrations indicated in figure legends, and then the cells were grown for 3 days.

Cell proliferation assay
NB cells were seeded in 96-well plates at a density of 10^3 cells per well in a final volume of 100 μl. The culture was maintained under 5% CO_2 and 10 μl WST-8 labeling solution (Cell counting Kit-8; DOJINDO, Kumamoto, Japan) was added, and the cells were returned to the incubator for 2 h. The absorbance of the formazan product formed was detected at 450 nm in a 96-well spectrophotometric plate reader, according to the manufacturer's protocol.

Western blot analysis
The cells were lysed in a buffer containing 5 mM EDTA, 2 mM Tris–HCl (pH 7.5), 10 mM β-glycerophosphate, 5 μg/ml aprotinin, 2 mM phenylmethylsulfonyl fluoride, 1 mM Na_3VO_4, protease inhibitor cocktail (Nacalai Tesque) and 1% SDS. Western blot analysis was performed as previously reported (Kurata *et al.*, 2008). After transferring to an Immobilon-P membrane (Millipore, Bedford, MA, USA), proteins were reacted with either anti-Bmi1 mouse monoclonal (229F6; Upstate, Charlottesville, VA, USA), anti-MYCN rabbit polyclonal (C-19; Santa Cruz, Santa Cruz, CA, USA) p14 (14P02; Oncogene) mouse, p16 (16P04; Neomarkers/Labvision, Fremont, CA, USA) mouse, anti-β-actin (Sigma-Aldrich) or a monoclonal anti-tubulin (Neomarkers Labvision) antibody. Anti-Ring1b mouse monoclonal antibodies were as described in a previous report (Atsuta *et al.*, 2001).

Immunohistochemistry
A 4-μm thick section of formalin-fixed, paraffin-embedded tissues was stained with hematoxylin and eosin and the adjacent sections were immunostained for Bmi1 using a polyclonal anti-Bmi1 antibody (AP2513c; ABGENT, San Diego, CA, USA). The Bench-Mark XT immunostainer (Ventana Medical Systems, Tucson, AZ, USA) and 3-3′ diaminobenzidine detection kit (Ventana Medical Systems) were used for visualization. Appropriate positive and negative control staining was also performed in parallel for each immunostaining. The tumor samples used in this study were kindly provided from various institutions and hospitals in Japan. Informed consent was obtained at each institution and hospital. All tumors were diagnosed clinically and pathologically as NBs and *MYCN* copy number was determined as previously described (Kurata *et al.*, 2008).

Semi-quantitative RT–PCR
The methods of semi-quantitative RT–PCR analysis were previously described (Kurata *et al.*, 2008). Total cellular RNA to prepare RT–PCR templates was extracted from NB cell lines using Isogen (Nippon Gene K K, Tokyo, Japan), and cDNA was synthesized from 1 μg total RNA templates according to the manufacturer's protocol (RiverTra-Ace-α RT–PCR kit; TOYOBO, Osaka, Japan). Primer sequences are described in Supplementary Table S1.

qPCR analysis for ChIP assay
qPCR analysis was performed using the ABI PRISM 7500 Real-Time PCR System (Applied Biosystems, Foster City, CA, USA), according to the manufacturer's instructions using SYBR Premix Dimer Eraser (Takara Bio, Ohtsu, Shiga, Japan). The primers for qPCR were designed and synthesized to produce 50–150 bp products. The primer sequence is listed in Supplementary Table S2. Each sample was amplified in triplicate. In Figure 3, the primer set was designed in E-box upstream of Bmi1 (Bmi1 promoter 1). In Figures 3, 6b, primer sets were designed in KIF1Bβ (KIF1B promoter 1, 2, 3) and TSLC1 (TSLC1 promoters 1, 2, 3).

Lentiviral infection
The packaging cell line HEK 293T (4×10^6) was plated and transfected the next day, when 1.5 μg of the transducing vectors containing the gene or shRNA, and 2.0 μg of the packaging vectors (Sigma-Aldrich) were cotransfected by the Fugene6 transfection reagent (Roche Applied Science, Indianapolis, IN, USA) according to the manufacturer's protocol. The medium was changed the next day and cells were cultured for another 24 h. Conditioned medium was then collected and cleared of debris by filtering through a 0.45-μm filter (Millipore). Thereafter, 1×10^5 NB cells were seeded in each well of a 6-well plate, and transduced by lentiviral-conditioned media. Transduced cells were analyzed by western blotting and RT–PCR.

Overexpression and knockdown of Bmi1
For the overexpression of Bmi1, FLAG-tagged mBmi1 plasmid was subcloned into lentivirus vector pHR-SIN-DL1. Cells were cultured in RPMI1640 and pooled. The pLKO.1-puromycin-based lentiviral vectors containing five sequence-verified shRNAs targeting human Bmi1 (RefSeq NM_005180) were obtained from the MISSION TRC-Hs 1.0 (Human) shRNA library (Sigma-Aldrich). Virus production, infection and selection were performed according to the manufacturer's protocol. At 1 week post infection, cells

were harvested and knockdown efficiency was assessed by western blotting. We checked Bmi1 knockdown by the five lentivirus-produced shRNAs and used two for experiments.

Luciferase reporter assay

The −1070/+53, −196/+53, −196/−122, −196/−122/mut (E-box sequence CACGTG changed to CA-G-G), −1070/+53 5′-upstream fragments were subcloned into luciferase reporter plasmid pGL4.17 (luc2/Neo) Luciferase Reporter Vector (Promega, Madison, WI, USA).

Tet21/N and SK-N-DZ cells were seeded in a 12-well plate 24 h before transfection at a concentration of 5×10^4 cells per well. Cells were cotransfected with Renilla luciferase reporter plasmid (pRL-TK, 10 ng) and luciferase reporter plasmid with the 5′-upstream region of the Bmi1 gene. The total amount of plasmid DNA per transfection was kept constant (510 ng) with pBlueScript KS+ by Lipofectamine 2000 (Invitrogen). At 48 h after transfection, cells were lysed and their luciferase activities were measured by the Dual-Luciferase reporter system (Promega). The rey luminescence signal was normalized on the basis of the Renilla luminescence signal.

ChIP assay

ChIP assay was performed as described previously (Orlando *et al.*, 1997, Fujimura *et al.*, 2006). Cross-linked chromatin prepared from the indicated cells was precipitated with normal mouse IgG (eBioscience, San Diego, CA, USA), monoclonal anti-MYCN antibody (NCMII100; Calbiochem, San Diego, CA, USA) or anti-Flag antibody (M2; Sigma-Aldrich). 'Input' DNA was isolated from the initial lysates of genomic DNA. Species-matched immunoglobulin-immunoprecipitated DNA (IgG), derived from the same volume of the chromatin fraction used for specific antibody immunoprecipitation, was subjected to PCR. Primers used in this study are listed in Supplementary Table S2. Each series of experiments was conducted at least three times.

cDNA microarray experiments

For gene expression profiling, in-house cDNA microarray with 13 440 spots was used. In all, 10 μg each of total RNA were labeled with the CyScribe RNA labeling kit in accordance with the manufacturer's manual (GE healthcare, Little Chalfont, Buckinghamshire, UK), followed by probe purification using the Qiagen MinElute PCR purification kit (Qiagen, Valencia, CA, USA). We used a mixture of RNAs isolated from eight human adult cancer cell lines as a common reference. RNAs from Bmi1-infected SK-N-BE and mock-infected SK-N-BE cells were labeled with Cy3 dye and a reference RNA mixture was labeled with Cy5 dye, mixed, and used as probes together with yeast tRNA and polyA for suppression. Subsequent hybridization and washing were conducted as described previously (Ohira *et al.*, 2005). Hybridized microarrays were scanned using the Agilent G2505A confocal laser scanner (Agilent technology, Santa Clara, CA, USA), and fluorescent intensities were quantified using the GenePix Pro microarray analysis software (Axon Instrument, Foster City, CA, USA). The resulting relative expression values for the gene spots were compared between Bmi1-infected and mock-infected SK-N-BE cells

Conflict of interest

The authors declare no conflict of interest.

Acknowledgements

We thank K Sakurai for technical assistance, and Daniel Mrozek, Medical English Service, for editorial assistance. This study was supported in part by a grant-in-aid from the Sankyo Foundation of Life Science, a grant-in-aid from the Ministry of Health, Labor, and Welfare for Third Term Comprehensive Control Research for Cancer, a grant-in-aid for Cancer Research (20–13) from the Ministry of Health, Labor, and Welfare of Japan, and a grant-in-aid from the Ministry of Education, Culture, Sports, Science and Technology, Japan.

References

Ando K, Ohira M, Ozaki T, Nakagawa A, Akazawa K, Suenaga Y *et al.* (2008). Expression of TSLC1, a candidate tumor suppressor gene mapped to chromosome 11q23, is downregulated in unfavorable neuroblastoma without promoter hypermethylation. *Int J Cancer* **123**: 2087–2094.

Atsuta T, Fujimura S, Moriya H, Vidal M, Akasaka T, Koseki H. (2001). Production of monoclonal antibodies against mammalian Ring1B proteins. *Hybridoma* **20**: 43–46.

Brodeur GM, Seeger RC, Schwab M, Varmus HE, Bishop JM. (1984). Amplification of N-myc in untreated human neuroblastomas correlates with advanced disease stage. *Science* **224**: 1121–1124.

Bruggeman SW, Hulsman D, Tanger E, Buckle T, Blom M, Zevenhoven J *et al.* (2007). Bmi1 controls tumor development in an Ink4a/Arf-independent manner in a mouse model for glioma. *Cancer Cell* **12**: 328–341.

Cao R, Tsukada Y, Zhang Y. (2005). Role of Bmi-1 and Ring1A in H2A ubiquitylation and Hox gene silencing. *Mol Cell* **20**: 845–854.

Caron H. (1995). Allelic loss of chromosome 1 and additional chromosome 17 material are both unfavourable prognostic markers in neuroblastoma. *Med Pediatr Oncol* **24**: 215–221.

Carén H, Ejeskär K, Fransson S, Hesson L, Latif F, Sjöberg RM *et al.* (2005). A cluster of genes located in 1p36 are down-regulated in neuroblastomas with poor prognosis, but not due to CpG island methylation. *Mol Cancer* **4**: 10.

Cui H, Ma J, Ding J, Li T, Alam G, Ding HF. (2006). Bmi-1 regulates the differentiation and clonogenic self-renewal of I-type neuroblastoma cells in a concentration-dependent manner. *J Biol Chem* **281**: 34696–34704.

Cui H, Hu B, Li T, Ma J, Alam G, Gunning WT *et al.* (2007). Bmi-1 is essential for the tumorigenicity of neuroblastoma cells. *Am J Pathol* **170**: 1370–1378.

Easton J, Wei T, Lahti JM, Kidd VJ. (1998). Disruption of the cyclin D/cyclin-dependent kinase/INK4/retinoblastoma protein regulatory pathway in human neuroblastoma. *Cancer Res* **58**: 2624–2632.

Esteller M. (2007). Cancer epigenomics: DNA methylomes and histone-modification maps. *Nat Rev Genet* **8**: 286–298.

Fujimura Y, Isono K, Vidal M, Endoh M, Kajita H, Mizutani-Koseki Y *et al.* (2006). Distinct roles of Polycomb group gene products in transcriptionally repressed and active domains of Hoxb8. *Development* **133**: 2371–2381.

Guney I, Wu S, Sedivy JM. (2006). Reduced c-Myc signaling triggers telomere-independent senescence by regulating Bmi-1 and p16(INK4a). *Proc Natl Acad Sci USA* **103**: 3645–3650.

Hanahan D, Weinberg RA. (2000). The hallmarks of cancer. *Cell* **100**: 57–70.

Iwama A, Oguro H, Negishi M, Kato Y, Morita Y, Tsukui H *et al.* (2004). Enhanced self-renewal of hematopoietic stem cells mediated by the polycomb gene product Bmi-1. *Immunity* **21**: 843–851.

Jacobs JJ, Kieboom K, Marino S, DePinho RA, van Lohuizen M. (1999). The oncogene and Polycomb-group gene bmi-1 regulates cell proliferation and senescence through the ink4a locus. *Nature* **397**: 164–168.

Jones PA, Baylin SB. (2002). The fundamental role of epigenetic events in cancer. *Nat Rev Genet* **3**: 415–428.

Kamminga LM, Bystrykh LV, de Boer A, Houwer S, Douma J, Weersing E *et al.* (2005). The Polycomb group gene Ezh2 prevents hematopoietic stem cell exhaustion. *Blood* **107**: 2170–2179.

Kamminga LM, de Haan G. (2006). Cellular memory and hematopoietic stem cell aging. *Stem Cells* **24**: 1143–1149.

Kramps C, Strieder V, Sapetschnig A, Suske G, Lutz W. (2004). E2F and Sp1/Sp3 synergize but are not sufficient to activate the *MYCN* gene in neuroblastomas. *J Biol Chem* **279**: 5110–5117.

Kurata K, Yanagisawa R, Ohira M, Kitagawa M, Nakagawara A, Kamijo T. (2008). Stress via p53 pathway causes apoptosis by mitochondrial Noxa upregulation in doxorubicin-treated neuroblastoma cells. *Oncogene* **27**: 741–754.

Lessard J, Sauvageau G. (2003). Bmi-1 determines the proliferative capacity of normal and leukaemic stem cells. *Nature* **423**: 255–260.

Leung C, Lingbeek M, Shakhova O, Liu J, Tanger E, Saremaslani P *et al.* (2004). Bmi1 is essential for cerebellar development and is overexpressed in human medulloblastomas. *Nature* **428**: 337–341.

Lutz W, Stohr M, Schurmann J, Wenzel A, Lohr A, Schwab M. (1996). Conditional expression of N-myc in human neuroblastoma cells increases expression of alpha-prothymosin and ornithine decarboxylase and accelerates progression into S-phase early after mitogenic stimulation of quiescent cells. *Oncogene* **13**: 803–812.

Molofsky AV, Pardal R, Iwashita T, Park IK, Clarke MF, Morrison SJ. (2003). Bmi-1 dependence distinguishes neural stem cell self-renewal from progenitor proliferation. *Nature* **425**: 962–967.

Molofsky AV, Slutsky SG, Joseph NM, He S, Pardal R, Krishnamurthy J *et al.* (2006). Increasing p16INK4a expression decreases forebrain progenitors and neurogenesis during ageing. *Nature* **443**: 448–452.

Munirajan AK, Ando K, Mukai A, Takahashi M, Suenaga Y, Ohira M *et al.* (2008). KIF1Bbeta functions as a haploinsufficient tumor suppressor gene mapped to chromosome 1p36.2 by inducing apoptotic cell death. *J Biol Chem* **283**: 24426–24434.

Murakami Y. (2005). Involvement of a cell adhesion molecule, TSLC1/IGSF4, in human oncogenesis. *Cancer Sci* **96**: 543–552.

Nowak K, Kerl K, Fehr D, Kramps C, Gessner C, Killmer K *et al.* (2006). BMI1 is a target gene of E2F-1 and is strongly expressed in primary neuroblastomas. *Nucleic Acids Res* **34**: 1745–1754.

Ohira M, Oba S, Nakamura Y, Isogai E, Kaneko S, Nakagawa A *et al.* (2005). Expression profiling using a tumor-specific cDNA microarray predicts the prognosis of intermediate risk neuroblastomas. *Cancer Cell* **7**: 337–350.

Orlando V, Strutt H, Paro R. (1997). Analysis of chromatin structure by *in vivo* formaldehyde cross-linking. *Methods* **11**: 205–214.

Pietersen AM, van Lohuizen M. (2008). Stem cell regulation by polycomb repressors: postponing commitment. *Curr Opin Cell Biol* **20**: 201–207.

Rajasekhar VK, Begemann M. (2007). Concise review: roles of polycomb group proteins in development and disease: a stem cell perspective. *Stem Cells* **25**: 2498–2510.

Schwartz YB, Pirrotta V. (2008). Polycomb complexes and epigenetic states. *Curr Opin Cell Biol* **20**: 266–273.

Sherr CJ. (2004). Principles of tumor suppression. *Cell* **116**: 235–246.

Sparmann A, van Lohuizen M. (2006). Polycomb silencers control cell fate, development and cancer. *Nat Rev Cancer* **6**: 846–856.

Strieder V, Lutz W. (2003). E2F proteins regulate MYCN expression in neuroblastomas. *J Biol Chem* **278**: 2983–2989.

Sugino Y, Misawa A, Inoue J, Kitagawa M, Hosoi H, Sugimoto T *et al.* (2007). Epigenetic silencing of prostaglandin E receptor 2 (PTGER2) is associated with progression of neuroblastomas. *Oncogene* **26**: 7401–7413.

Teitz T, Wei T, Valentine MB, Vanin EF, Grenet J, Valentine VA *et al.* (2000). Caspase 8 is deleted or silenced preferentially in childhood neuroblastomas with amplification of MYCN. *Nat Med* **6**: 529–535.

Valk-Lingbeek ME, Bruggeman SW, van Lohuizen M. (2004). Stem cells and cancer; the polycomb connection. *Cell* **118**: 409–418.

Viré E, Brenner C, Deplus R, Blanchon L, Fraga M, Didelot C *et al.* (2006). The Polycomb group protein EZH2 directly controls DNA methylation. *Nature* **439**: 871–874.

Westemann F, Schwab M. (2002). Genetic parameters of neuroblastomas. *Cancer Lett* **184**: 127–147.

Yan P, Mühlethaler A, Bourloud KB, Beck MN, Gross N. (2003). Hypermethylation-mediated regulation of CD44 gene expression in human neuroblastoma. *Gene Chromosomes Cancer* **36**: 129–138.

Yang Q, Zage P, Kagan D, Tian Y, Seshadri R, Salwen HR *et al.* (2004). Association of epigenetic inactivation of RASSF1A with poor outcome in human neuroblastoma. *Clin Cancer Res* **10**: 8493–8500.

Yang QW, Liu S, Tian Y, Salwen HR, Chlenski A, Weinstein J *et al.* (2003). Methylation-associated silencing of the thrombospondin-1 gene in human neuroblastoma. *Cancer Res* **63**: 6299–6310.

Yang J, Chai L, Liu F, Fink LM, Lin P, Silberstein LE *et al.* (2007). Bmi-1 is a target gene for SALL4 in hematopoietic and leukemic cells. *Proc Natl Acad Sci USA* **104**: 10494–10499.

Supplementary Information accompanies the paper on the Oncogene website (http://www.nature.com/onc)